Title	Theoretical chemical kinetic study of the h-atom abstraction reactions from aldehydes and acids by Atoms and H, H2, and H3 radicals
Author(s)	Mendes, Jorge; Zhou, Chong-Wen; Curran, Henry J.
Publication Date	2014-11-11
Publication Information	Mendes, J,Zhou, CW,Curran, HJ (2014) 'Theoretical chemical kinetic study of the h-atom abstraction reactions from aldehydes and acids by Atoms and H, H2, and H3 radicals'. Journal Of Physical Chemistry A, 118 :12089-12104.
Publisher	American Chemical Society
Link to publisher's version	http://dx.doi.org/10.1021/jp5072814
Item record	http://hdl.handle.net/10379/6149
DOI	http://dx.doi.org/10.1021/jp5072814

Theoretical Chemical Kinetic Study of the H-Atom Abstraction Reactions from Aldehydes and Acids by $\dot{H}$ Atoms and $\dot{O}H$, $H\dot{O}_2$ and $\dot{C}H_3$ Radicals

Jorge Mendes, Chong-Wen Zhou,* and Henry J. Curran

Combustion Chemistry Centre, National University of Ireland, Galway, Ireland.

E-mail: chongwen.zhou@nuigalway.ie

*To whom correspondence should be addressed

Abstract

We have performed a systematic, theoretical chemical kinetic investigation of H-atom abstraction by $\dot{H}$ atoms and $\dot{O}H$, $H\dot{O}_2$ and $\dot{C}H_3$ radicals from aldehydes (methanal, ethanal, propanal and isobutanal) and acids (methanoic acid, ethanoic acid, propanoic acid and isobutanoic acid). The geometry optimizations and frequencies of all of the species in the reaction mechanisms of the title reactions were calculated using the MP2 method and the 6-311G(d,p) basis set. The one dimensional hindered rotor treatment for reactants and transition states and the intrinsic reaction coordinate calculations were also determined at the MP2/6-311G(d,p) level of theory. For the reactions of methanal and methanoic acid with $\dot{H}$ atoms and $\dot{O}H$, $H\dot{O}_2$ and $\dot{C}H_3$ radicals, the calculated relative electronic energies were obtained with the CCSD(T)/cc-pV*X*Z (where X = D, T and Q) method and were extrapolated to the complete basis set (CBS) limit. The electronic energies obtained with the CCSD(T)/cc-pVTZ method were benchmarked against the CCSD(T)/CBS energies and were found to be within 1 kcal mol^{-1} of one another. Thus, the energies calculated using the less expensive CCSD(T)/cc-pVTZ method were used in all of the reaction mechanisms and in calculating our high-pressure limit rate constants for the title reactions. Rate constants were calculated using conventional transition state theory with an asymmetric Eckart tunneling correction, as implemented in Variflex. Herein, we report the individual and average rate constants, on a per H-atom basis, and total rate constants in the temperature range 500–2000 K. We have compared some of our rate constant results to available experimental and theoretical data and our results are generally in good agreement.

Keywords

ab-initio, hydrogen, hydroxyl, hydroperoxyl, methyl, formaldehyde, acetaldehyde, formic acid, acetic acid, rate constants

Introduction

Both aldehydes and acids are intermediate species in the reaction mechanisms of alkanes. Formaldehyde (CH_2O) and acetaldehyde (CH_3CHO) are the main aldehydes formed in many oxidation processes.[1] The most plentiful carboxylic acid in the troposphere is formic acid and its presence is due to processes such as the oxidation of volatile organic compounds, burning of biomass, engine emissions, among others.[2]

In combustion relevant conditions, hydrogen atom abstraction reactions by $\dot{H}$ atoms and $\dot{O}H$, $H\dot{O}_2$ and $\dot{C}H_3$ radicals vary in importance depending on the temperature ($\dot{O}H$: $>$ 500 K, $H\dot{O}_2$: 800$-$1300 K, $\dot{H}$ and $\dot{C}H_3$: $>$ 1300 K). In our previous works on alcohols,[3,4] ethers,[5,6] ketones[7–9] and esters[10,11] we have investigated the influence that the presence of the functional group has on the rate constants for abstraction of a hydrogen atom by $\dot{O}H$ and $H\dot{O}_2$ radicals. Herein we perform a similar systematic study of the hydrogen atom abstraction reactions from several aldehydes (methanal, ethanal, propanal and isobutanal) and acids (methanoic acid, ethanoic acid, propanoic acid and isopropanoic acid) by $\dot{H}$ atoms and $\dot{O}H$, $H\dot{O}_2$ and $\dot{C}H_3$ radicals in the temperature range 500–2000 K.

As in our previous works,[3–11] we have found a stepwise mechanism where reactant complexes are formed in the entrance channel and product complexes are formed in the exit channel when abstracting a hydrogen atom from aldehydes and acids by $\dot{O}H$, $H\dot{O}_2$ and $\dot{C}H_3$ radicals. In the case of H-atom abstraction by a $\dot{H}$ atom, reactant complexes are not formed in the entrance channel.

In our previous study of the hydrogen atom abstraction reactions from ketones by $\dot{O}H$ radicals,[7] two reactant conformers (gauche and trans) have been studied which have similar chemical properties. In a more recent study on esters + $H\dot{O}_2$ radicals[11] we have stated that the energy required for the rotation of the α'–β' and β'–γ' hindered rotors of methyl pentanoate is 4.5 and 5.7 kcal mol^{-1}, respectively, and that the relative energy of the gauche reactant conformer is 4 kcal mol^{-1} higher than that of the trans reactant conformer. Therefore, as in our previous studies[6,8–11] we only consider the trans reactant conformers when determining the structure of the transition states, which are shown in Figures 1 and 2.

In the specific case of acids, the structure of the lowest energy reactant conformer is where the OH group is aligned with the C=O group. The energy barrier for rotation of the $R'C(=O)-OH$ hindered rotor is about 14 kcal mol^{-1} where the relative energy of the other conformer is about 5 kcal mol^{-1} higher than that of the lowest energy conformer. Therefore, we only consider the lowest energy conformer in our calculations.

Methodology

Gaussian-09[12] with the second order Møller-Plesset (MP2) method and the 6-311G(d,p) basis set was used in the geometry optimizations, frequency calculations and external rotational constants for every species in the reaction mechanisms and hindered rotor potentials for reactants and transition states. Each transition state was connected to the corresponding local minimum on either side of the transition state on the potential energy surface, with the use of intrinsic reaction coordinate calculations.

For the reaction mechanisms of methanal and methanoic acid when undergoing abstraction of a hydrogen atom by $\dot{H}$ atoms and $\dot{O}H$, $H\dot{O}_2$ and $\dot{C}H_3$ radicals, the relative electronic energies have been calculated at the CCSD(T)/cc-pV*X*Z (where *X* = D, T and Q) level of theory and corresponding extrapolation to the complete basis set (CBS) limit.[13] The electronic energies calculated at the CCSD(T)/cc-pVTZ level were benchmarked against the ones calculated at the CBS limit and they are within 1 kcal mol^{-1} of each other. These were then used to calculate the high-pressure limit rate constant in this work. All energies have been reported as zero-point corrected electronic energies and all of the harmonic frequencies were scaled by 0.9496 as recommended by Merrick *et al.*[14] ChemCraft[15] has been used in the visualization and determination of geometrical parameters.

Our rate constants have been calculated using conventional transition state theory[16] with an asymmetric Eckart tunneling correction,[17] as implemented in Variflex v2.02m,[18] in the tempera-

ture range 500–2000 K:

$$k^{TST}(T) = \sigma\kappa\frac{k_B T}{h}\frac{Q^{\ddagger}(T)}{Q_A(T)Q_B(T)}\exp(-\frac{E^{\ddagger}}{k_B T}) \quad (1)$$

Where, $k^{TST}(T)$ is the rate constant at temperature T; σ is the reaction path degeneracy; κ is the asymmetric Eckart tunneling factor; k_B is the Boltzmann constant; h is the Planck constant; $Q^{\ddagger}(T)$ is the partition function for the transition state; $Q_A(T)$ and $Q_B(T)$ are the partition functions for the reactants and $E^{\ddagger}$ is the calculated electronic energy barrier height. Each partition function is evaluated with respect to the zero-point levels of reactants and transition states and are the product of translational (Q_{trans}), vibrational (Q_{vib}), external rotational (Q_{rot}), torsional (Q_{tor}) and electronic (Q_{el}) partition functions ($Q = Q_{trans}.Q_{vib}.Q_{rot}.Q_{tor}.Q_{el}$).

Potential Energy Surface

Figures 1 and 2 detail the optimized geometries of the aldehydes and acids studied, respectively, as well as the nomenclature used. Tables S1, S3, S5 and S7 of the Supplementary Information (SI) provide details of the CCSD(T)/cc-pVDZ (TZ, QZ) and CCSD(T)/CBS calculated relative electronic energies for the abstraction of a hydrogen atom by $\dot{H}$ atoms and $\dot{O}H$, $H\dot{O}_2$ and $\dot{C}H_3$ radicals, respectively, from methanal and methanoic acid. Tables S2, S4, S6 and S8 of the SI provides the geometry co-ordinates and frequencies for the reactants and transitions states in the title reactions.

Table 1 details the calculated relative electronic energies of the transition states for H-atom abstraction $\dot{H}$ atoms from aldehydes and acids. Figures 3(a)−3(d) and Figures 4(a)−4(d) detail the corresponding potential energy surfaces (PES) for aldehydes and acids, respectively.

Figure 3(a) shows the PES for the H-atom abstraction reactions of methanal + $\dot{H}$ atoms calculated with the CCSD(T)/cc-pVTZ and CCSD(T)/CBS (in parentheses) methods, in kcal mol^{-1}. Figures 3(b)–3(d) show the PES calculated using the CCSD(T)/cc-pVTZ method for the reactions of ethanal (Figure 3(b)), propanal (Figure 3(c)) and isobutanal (Figure 3(d)), in kcal mol^{-1}. Ab-

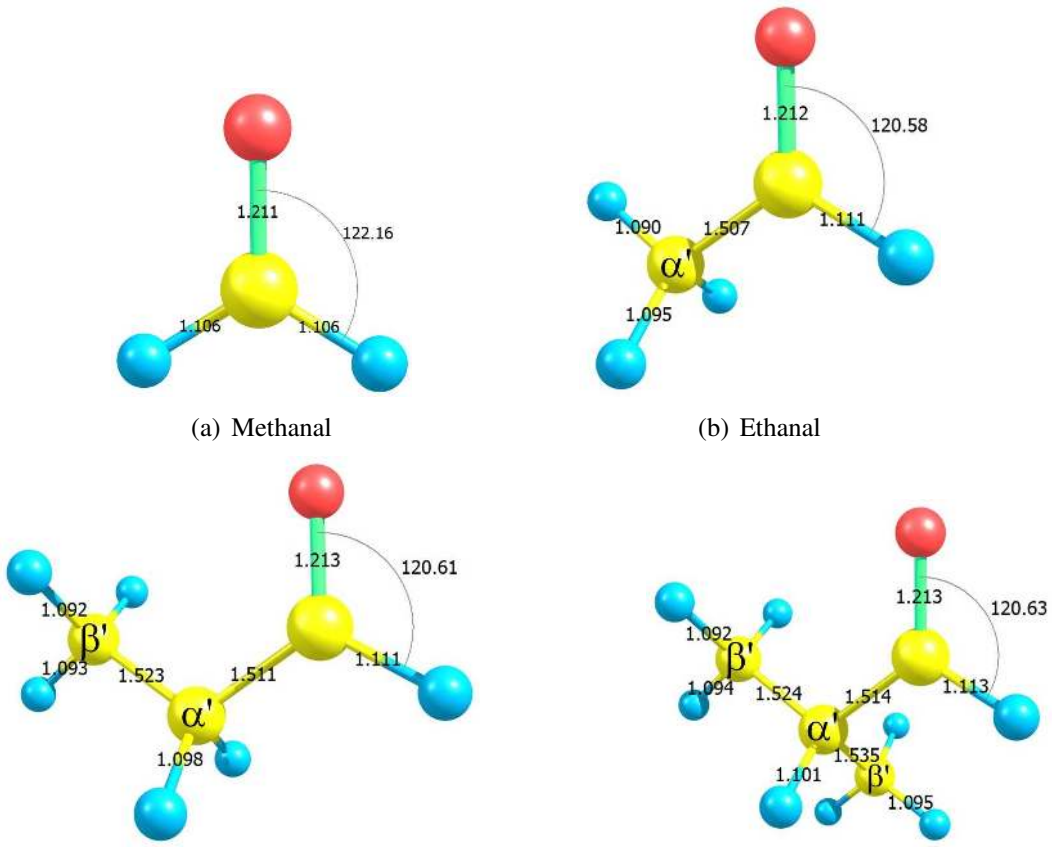

(a) Methanal (b) Ethanal

(c) Propanal (d) Isobutanal

Figure 1: Optimized geometries of the aldehydes in this work at MP2/6-311G(d,p) level of theory, detailing the different labels we use.

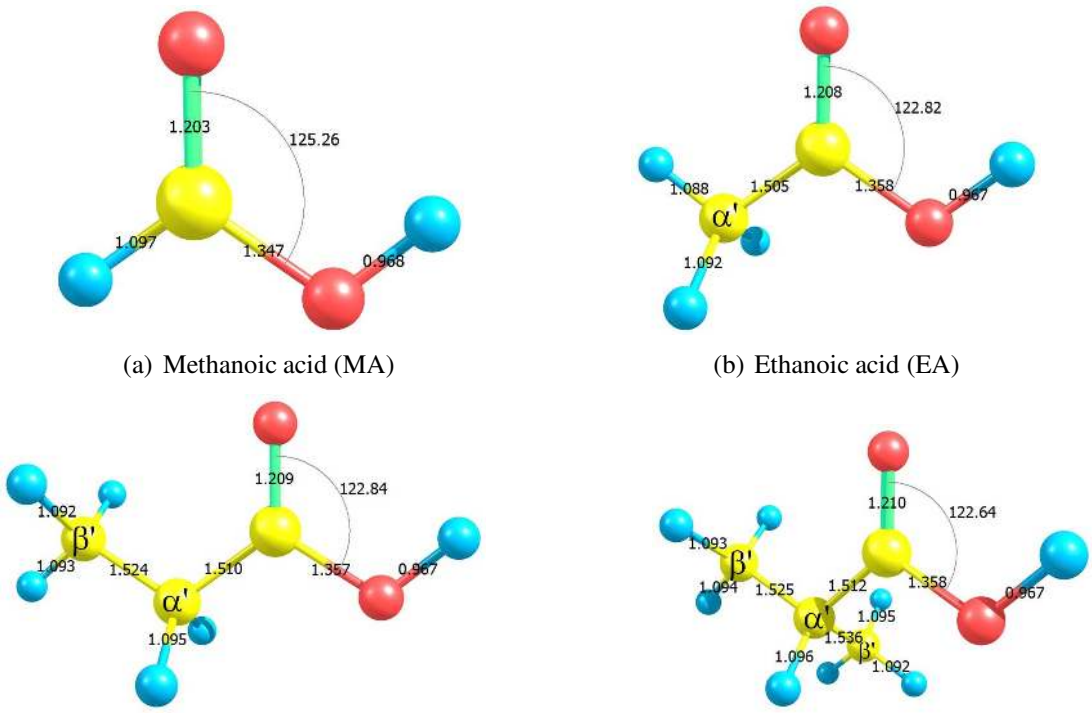

(a) Methanoic acid (MA)

(b) Ethanoic acid (EA)

(c) Propanoic acid (PA)

(d) Isobutanoic acid (iBA)

Figure 2: Optimized geometries of the acids in this work at MP2/6-311G(d,p) level of theory, detailing the different labels we use.

straction of a H-atom by a $\dot{H}$ atom occurs similarly for all of the aldehydes studied. The formation of a reactant complex is not observed in the entrance channel and a transition state is formed directly from reactants at each position relative to the functional group. The transition state for abstracting the aldehylic (R′C(=O)–H) hydrogen atom has a calculated relative electronic energy of 7 kcal mol^{-1} for methanal and 5 kcal mol^{-1} for ethanal, propanal and isobutanal, Table 1. Abstracting an α' hydrogen atom has calculated relative electronic energies for the transition state of 12, 9 and 7 kcal mol^{-1} for ethanal, propanal and isobutanal, respectively. Abstraction of a β' hydrogen atom has a relative energy of 12 kcal mol^{-1} for both propanal and isobutanal. Product complexes are formed in the exit channels, followed by the products.

Figure 4(a) shows the PES for H-atom abstraction reactions from methanoic acid by $\dot{H}$ atoms calculated with the CCSD(T)/cc-pVTZ and CCSD(T)/CBS (in parentheses) methods, in kcal mol^{-1}. Figures 4(b)–4(d) show the PES, in kcal mol^{-1}, calculated using the CCSD(T)/cc-pVTZ method for the reactions of ethanoic acid, Figure 4(b), propanoic acid, Figure 4(c) and isobutanoic acid, Figure 4(d). As for aldehydes, abstraction of a hydrogen atom by a $\dot{H}$ atom occurs similarly for all of the acids studied where abstracting the acidic (R′C(=O)O–H) hydrogen atom has a calculated relative electronic energy for the transition states of $17-18$ kcal mol^{-1} for all of the acids studied. Abstracting the C–H hydrogen atom in methanoic acid has a relative energy of 11 kcal mol^{-1} while abstracting a hydrogen atom at the α' position has calculated relative electronic energies of 11, 8 and 7 kcal mol^{-1} for ethanoic acid, propanoic acid and isobutanoic acid, respectively. Abstraction of a β' hydrogen atom has a relative energy of 12 kcal mol^{-1} for both propanoic acid and isobutanoic acid. Product complexes are also formed in the exit channel before forming the products.

Abstraction of a hydrogen atom by $\dot{O}H$, $H\dot{O}_2$ and $\dot{C}H_3$ radicals at each position of the aldehydes and acids begins with the formation of a reactant complex in the entrance channel which was not observed when undergoing abstraction by $\dot{H}$ atoms. In the case of $\dot{O}H$ and $H\dot{O}_2$ radicals, this reactant complex forms a hydrogen bond between the H-atom of the radical and the oxygen atom of the functional group. Moreover, with $\dot{C}H_3$ radicals the formation of this complex is due

to a very weak van der Waals interaction between the radical and the oxygenated molecule. It then proceeds through a transition state before forming a product complex in the exit channel, ultimately leading to products. Tables 2, 3 and 4 detail the calculated relative electronic energies of the transition states for abstraction of a hydrogen atom from aldehydes and acids by $\dot{O}H$, $H\dot{O}_2$ and $\dot{C}H_3$ radicals, respectively. Figures 5(a)−10(d) show the PES for aldehydes (5(a)−5(d), 7(a)−7(d) and 9(a)−9(d)) and acids (6(a)−6(d), 8(a)−8(d) and 10(a)−10(d)) when reacting with these radicals.

Figures 5(a) and 6(a) show the PES, in kcal mol^{-1}, for abstraction of a H-atom by $\dot{O}H$ radicals from methanal and methanoic acid, respectively, calculated with the CCSD(T)/cc-pVTZ and CCSD(T)/CBS (in parentheses) methods. Figures 5(b)–5(d) and Figures 6(b)–6(d) show the PES calculated using the CCSD(T)/cc-pVTZ method when a $\dot{O}H$ radical abstracts a hydrogen atom from ethanal (Figure 5(b)), propanal (Figure 5(c)), isobutanal (Figure 5(d)), ethanoic acid (Figure 6(b)), propanoic acid (Figure 6(c)) and isobutanoic acid (Figure 6(d)), in kcal mol^{-1}. When an $\dot{O}H$ radical reacts with aldehydes and acids reactant complexes are formed in the entrance channel with relative electronic energies ranging from -5.0 to -3.9 and -8.0 to -3.1 kcal mol^{-1}, respectively. A transition state is then formed for abstraction of a hydrogen atom at each position with relative energies ranging from -3.2 to 3.3 kcal mol^{-1} and -0.3 to 4.2 kcal mol^{-1} for aldehydes and acids, respectively. Product complexes are then formed in the exit channel followed by the products.

Figures 7(a) and 8(a) show the PES, in kcal mol^{-1}, for the abstraction of a hydrogen atom by $H\dot{O}_2$ radicals from methanal and methanoic acid, respectively, calculated with the CCSD(T)/cc-pVTZ and CCSD(T)/CBS (in parentheses) methods. Figures 7(b)–7(d) and Figures 8(b)–8(d) show the PES calculated using the CCSD(T)/cc-pVTZ method when a $H\dot{O}_2$ radical abstracts a hydrogen atom from ethanal (Figure 7(b)), propanal (Figure 7(c)), isobutanal (Figure 7(d)), ethanoic acid (Figure 8(b)), propanoic acid (Figure 8(c)) and isobutanoic acid (Figure 8(d)), in kcal mol^{-1}. As with $\dot{O}H$ radicals, when a $H\dot{O}_2$ radical reacts with aldehydes and acids, reactant complexes are also formed in the entrance channel with energies ranging from -8.8 to -7.3 kcal mol^{-1} and -14.4 to

-4.1 kcal mol^{-1}, respectively. The formation of the transition states follows with relative energies ranging from 11.0 to 22.1 kcal mol^{-1} and 14.7 to 25.6 kcal mol^{-1}, respectively. Product complexes are also formed in the exit channel followed by the products.

Figures 9(a) and 10(a) show the PES, in kcal mol^{-1}, for the abstraction of a hydrogen atom by $\dot{C}H_3$ radicals from methanal and methanoic acid, respectively, calculated with the CCSD(T)/cc-pVTZ and CCSD(T)/CBS (in parentheses) methods. Figures 9(b)–9(d) and Figures 10(b)–10(d) show the PES calculated using the CCSD(T)/cc-pVTZ method when undergoing abstraction of a hydrogen atom by $\dot{C}H_3$ radicals from ethanal (Figure 9(b)), propanal (Figure 9(c)), isobutanal (Figure 9(d)), ethanoic acid (Figure 10(b)), propanoic acid (Figure 10(c)) and isobutanoic acid (Figure 10(d)), in kcal mol^{-1}. Reactant complexes are also formed when $\dot{C}H_3$ radicals react with aldehydes and acids, although with a much weaker interaction than with $\dot{O}H$ and $H\dot{O}_2$ radicals, having relative energies ranging from -1.0 to -0.6 kcal mol^{-1} and -2.0 to -0.8 kcal mol^{-1}, respectively. The transition states have relative energies ranging from 9.2 to 15.0 kcal mol^{-1} and 9.4 to 14.9 kcal mol^{-1} for aldehydes and acids, respectively, followed by the product complexes and products.

Table 1: Calculated electronic energies (in kcal mol^{-1}) of the transition states relative to the reactants for aldehydes and acids + $\dot{H}$ atoms in this work, detailing the different types of hydrogen atoms present.

Species			β'	α'		R′CO–H
(a)	Methanal	CH_2O				7.0
(b)	Ethanal	CH_3CHO		11.7 (1°)		5.3
(c)	Propanal	CH_3CH_2CHO	11.6 (1°)	8.9 (2°)		5.0
(d)	Isobutanal	$(CH_3)_2CHCHO$	11.8 (1°)	6.6 (3°)		4.7
					H–C(=O)OH	R′C(=O)O–H
(e)	Methanoic acid (MA)	HC(=O)OH			11.1	17.3
(f)	Ethanoic acid (EA)	$CH_3C(=O)OH$		11.2 (1°)		18.0
(g)	Propanoic acid (PA)	$CH_3CH_2C(=O)OH$	11.7 (1°)	8.4 (2°)		17.9
(h)	Isobutanoic acid (iBA)	$(CH_3)_2CHC(=O)OH$	11.7 (1°)	6.5 (3°)		16.9

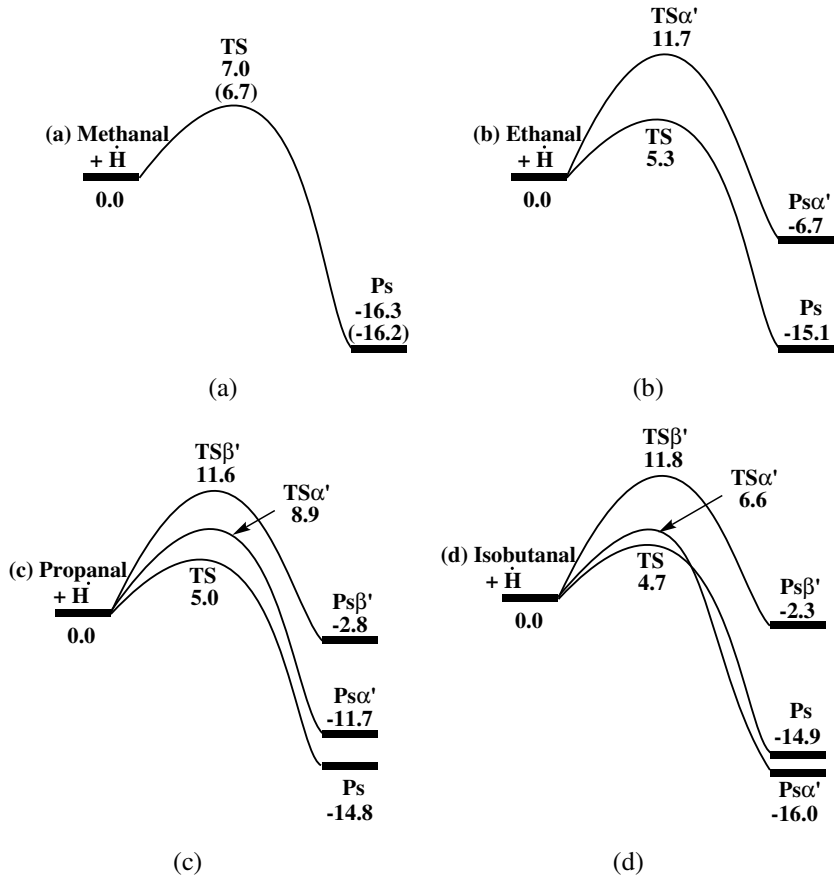

Figure 3: PES of the reactions of aldehydes with Ḣ atoms calculated with the CCSD(T)/cc-pVTZ and CCSD(T)/CBS (in parentheses) methods for (a) methanal and calculated with the CCSD(T)/cc-pVTZ method for (b) ethanal, (c) propanal and (d) isobutanal, in kcal mol^{-1}.

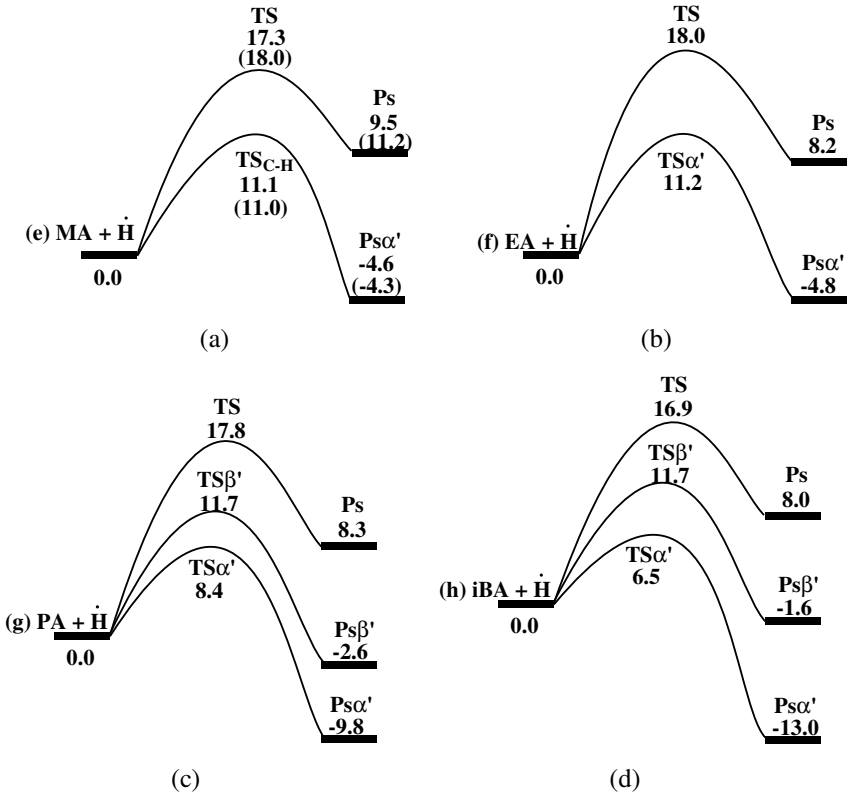

Figure 4: PES of the reactions of acids with Ḣ atoms calculated with the CCSD(T)/cc-pVTZ and CCSD(T)/CBS (in parentheses) methods for (a) methanoic acid and calculated with the CCSD(T)/cc-pVTZ method for (b) ethanoic acid, (c) propanoic acid and (d) isobutanoic acid, in kcal mol^{-1}.

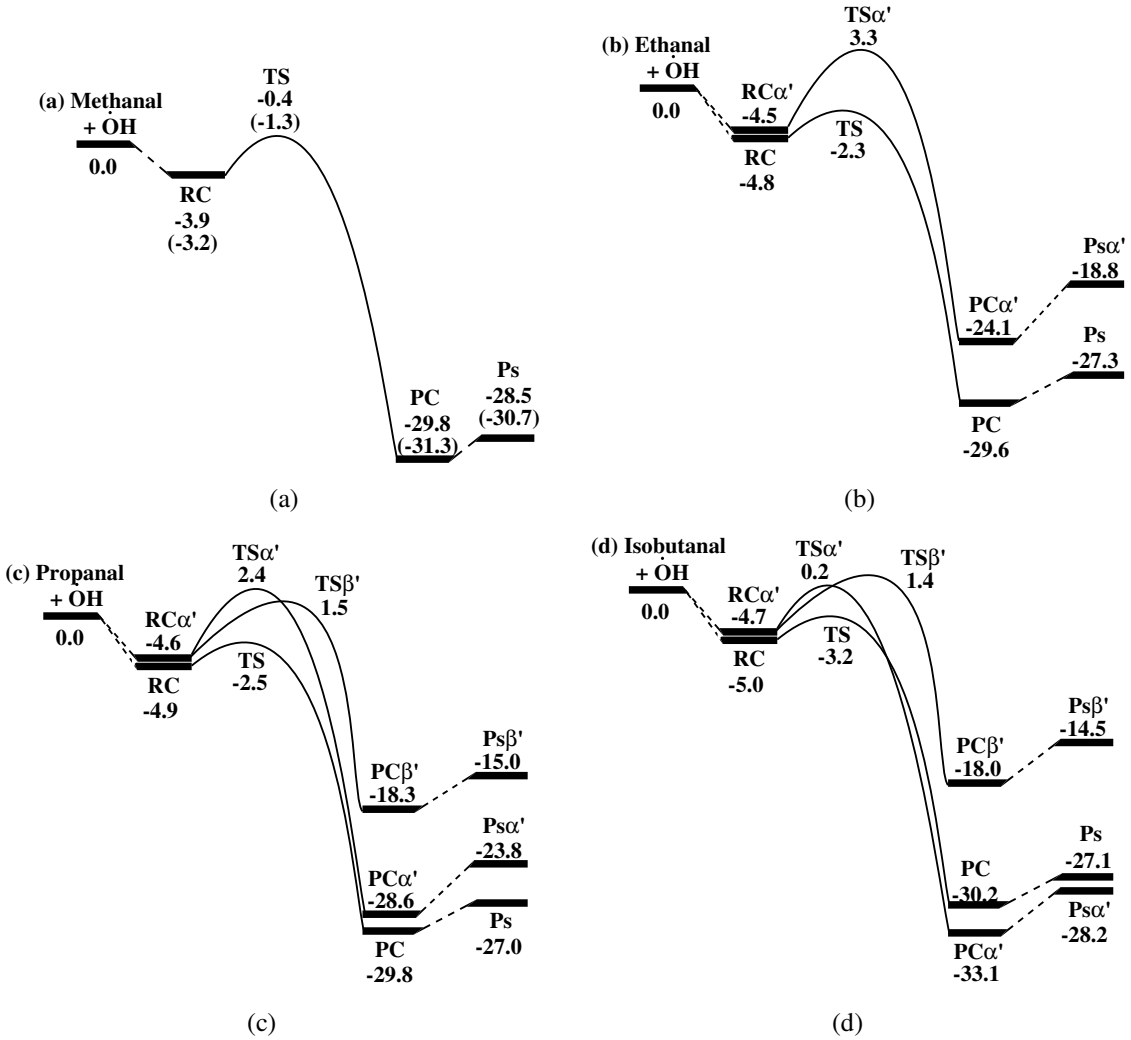

Figure 5: PES of the reactions of aldehydes with $\dot{O}H$ radicals calculated with the CCSD(T)/cc-pVTZ and CCSD(T)/CBS (in parentheses) methods for (a) methanal and calculated with the CCSD(T)/cc-pVTZ method for (b) ethanal, (c) propanal and (d) isobutanal, in kcal mol^{-1}.

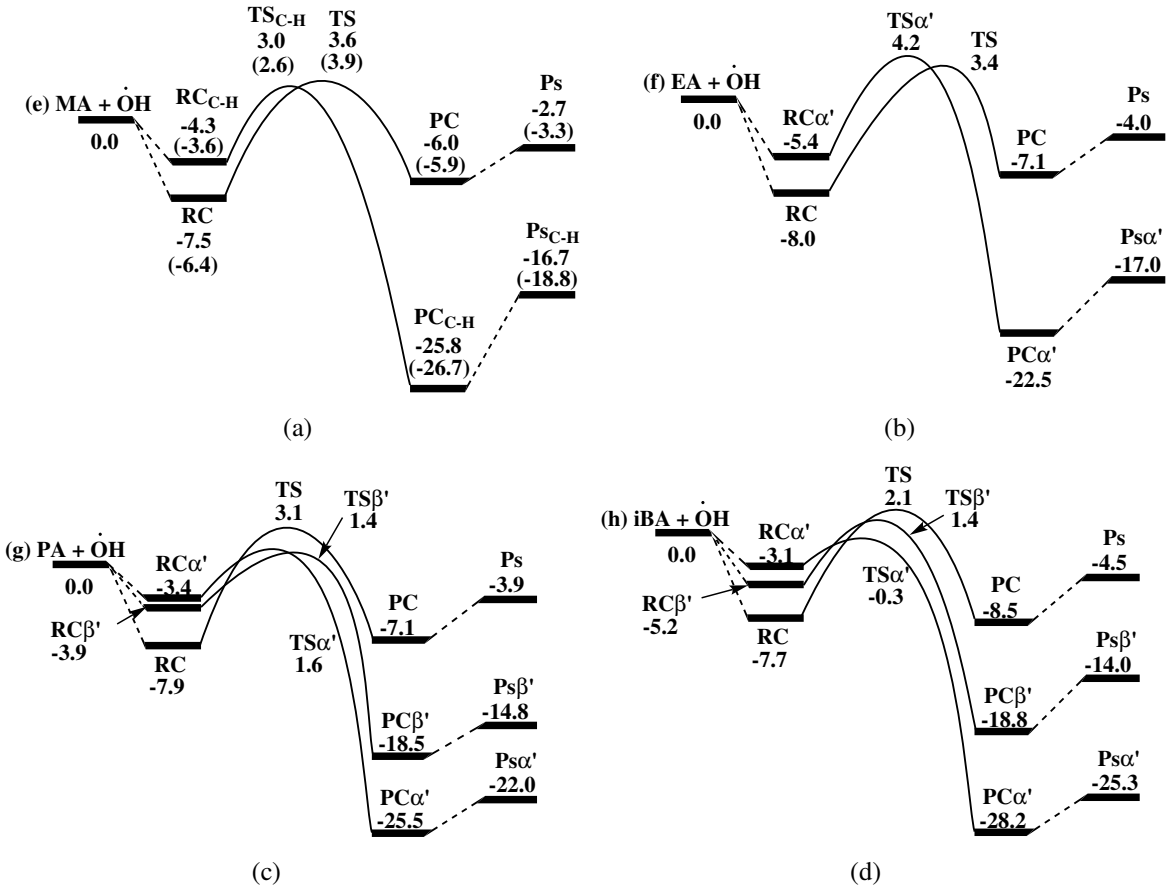

Figure 6: PES of the reactions of acids with ȮH radicals calculated with the CCSD(T)/cc-pVTZ and CCSD(T)/CBS (in parentheses) methods for (a) methanoic acid and calculated with the CCSD(T)/cc-pVTZ method for (b) ethanoic acid, (c) propanoic acid and (d) isobutanoic acid, in kcal mol^{-1}.

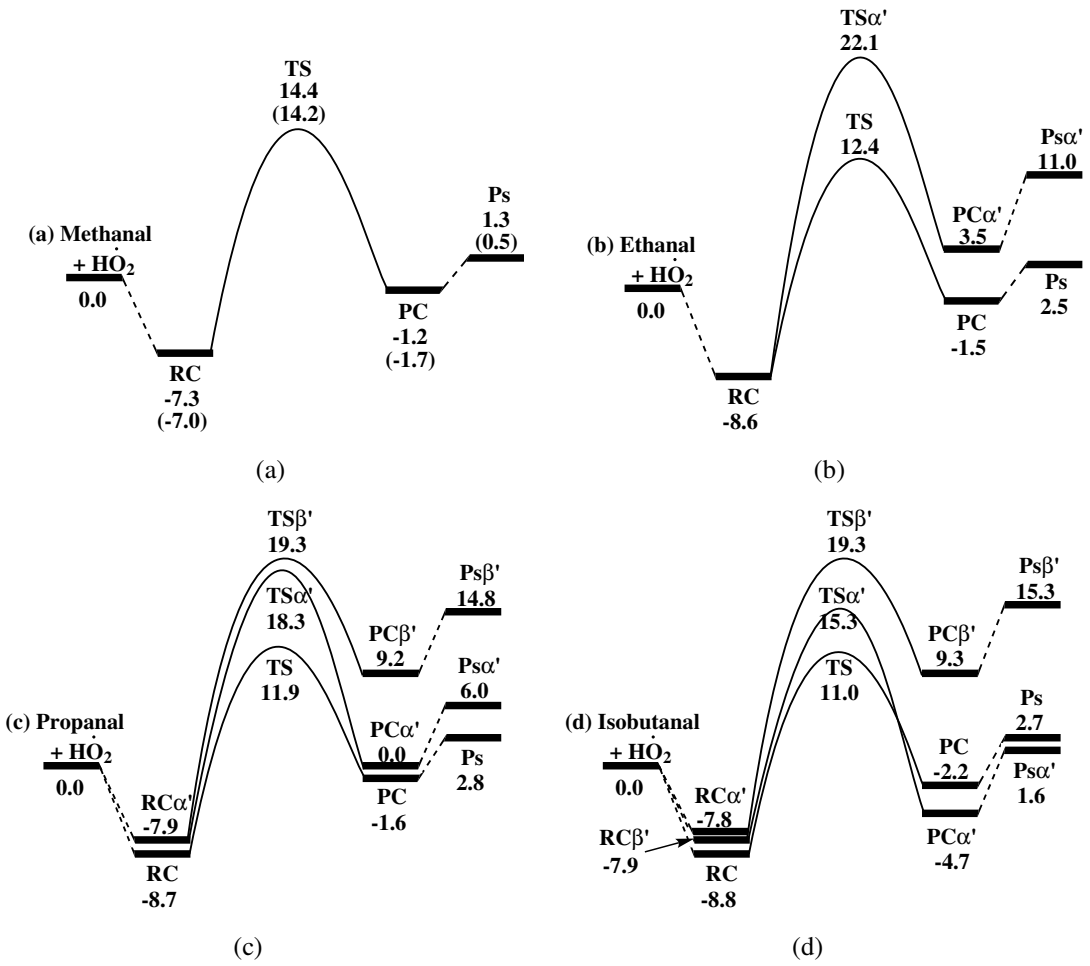

Figure 7: PES of the reactions of aldehydes with $H\dot{O}_2$ radicals calculated with the CCSD(T)/cc-pVTZ and CCSD(T)/CBS (in parentheses) methods for (a) methanal and calculated with the CCSD(T)/cc-pVTZ method for (b) ethanal, (c) propanal and (d) isobutanal, in kcal mol^{-1}.

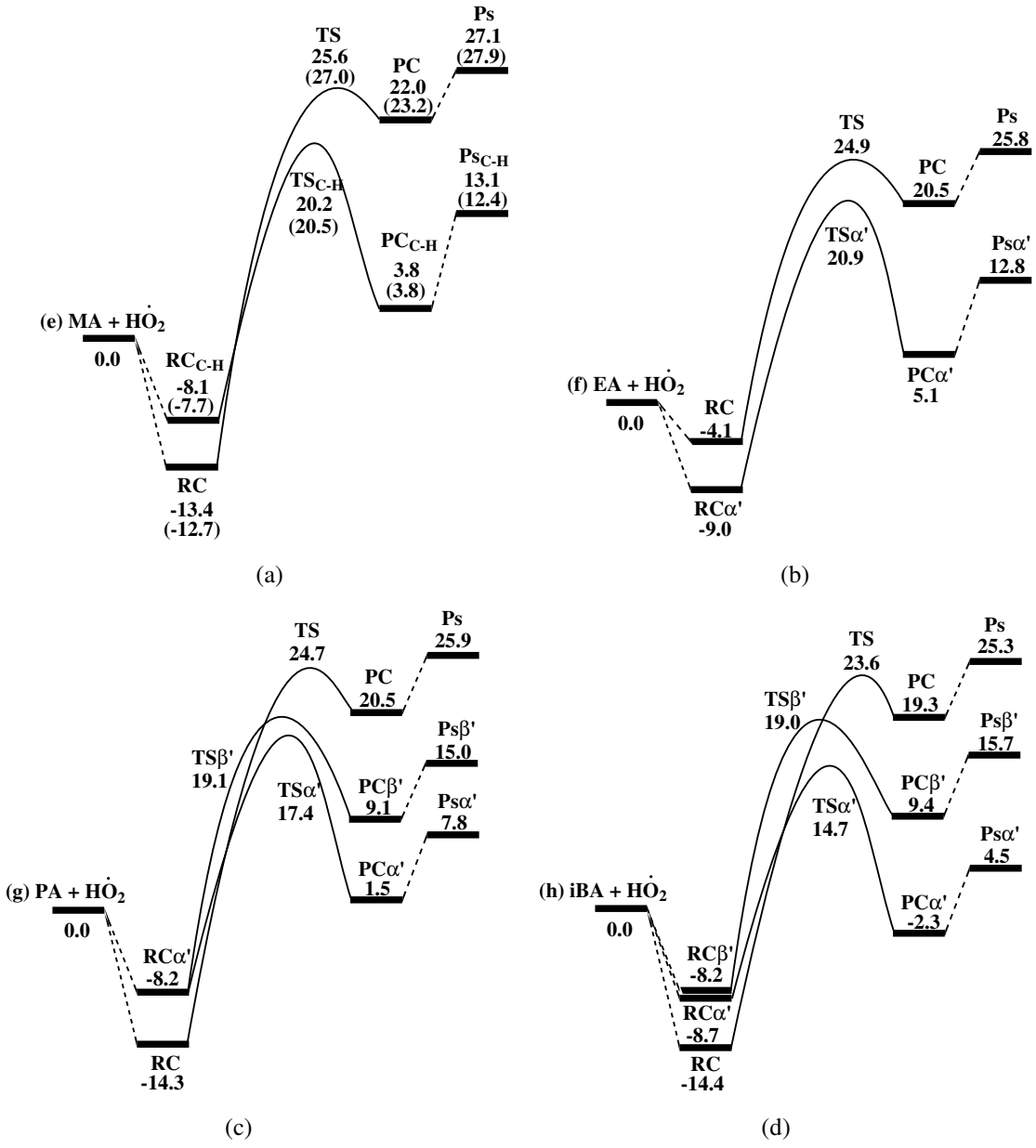

Figure 8: PES of the reactions of acids with $H\dot{O}_2$ radicals calculated with the CCSD(T)/cc-pVTZ and CCSD(T)/CBS (in parentheses) methods for (a) methanoic acid and calculated with the CCSD(T)/cc-pVTZ method for (b) ethanoic acid, (c) propanoic acid and (d) isobutanoic acid, in kcal mol^{-1}.

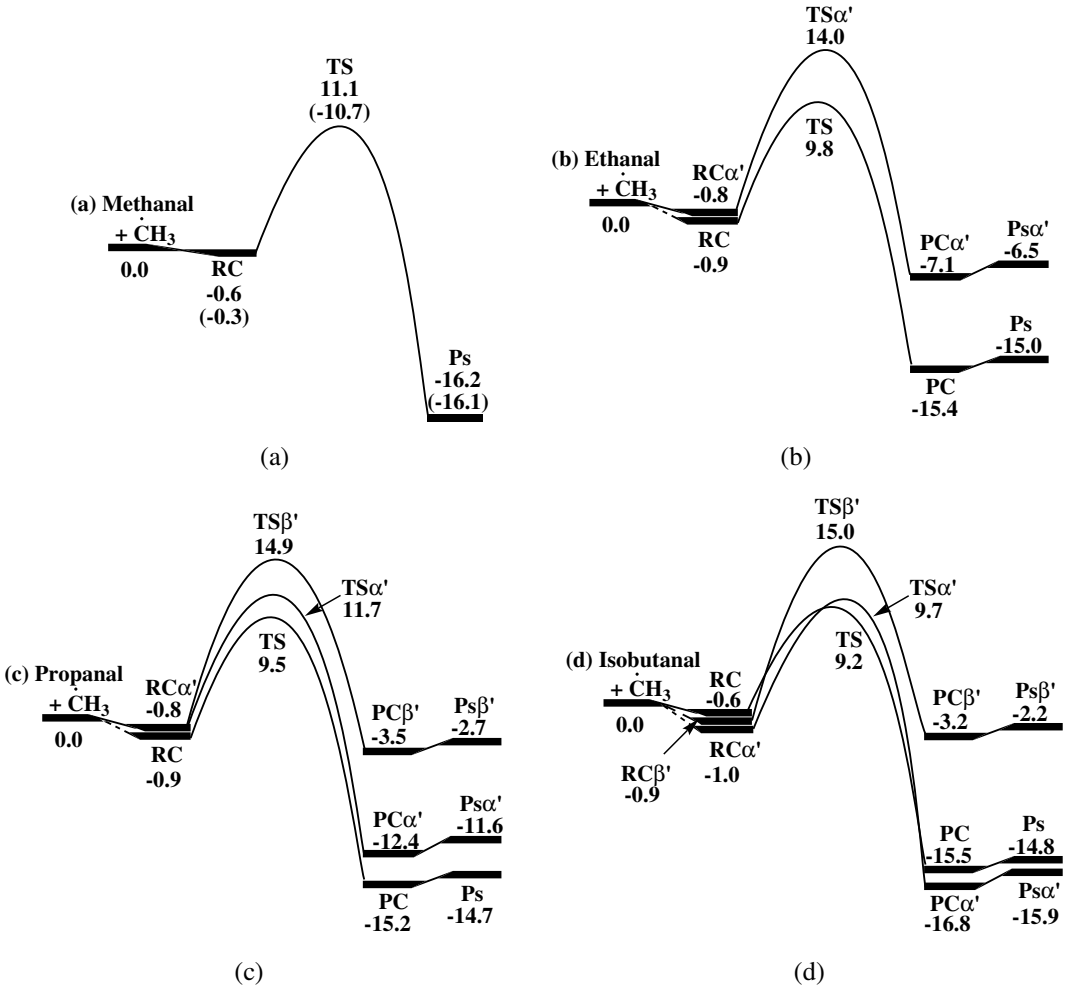

Figure 9: PES of the reactions of aldehydes with $\dot{C}H_3$ radicals calculated with the CCSD(T)/cc-pVTZ and CCSD(T)/CBS (in parentheses) methods for (a) methanal and calculated with the CCSD(T)/cc-pVTZ method for (b) ethanal, (c) propanal and (d) isobutanal, in kcal mol^{-1}.

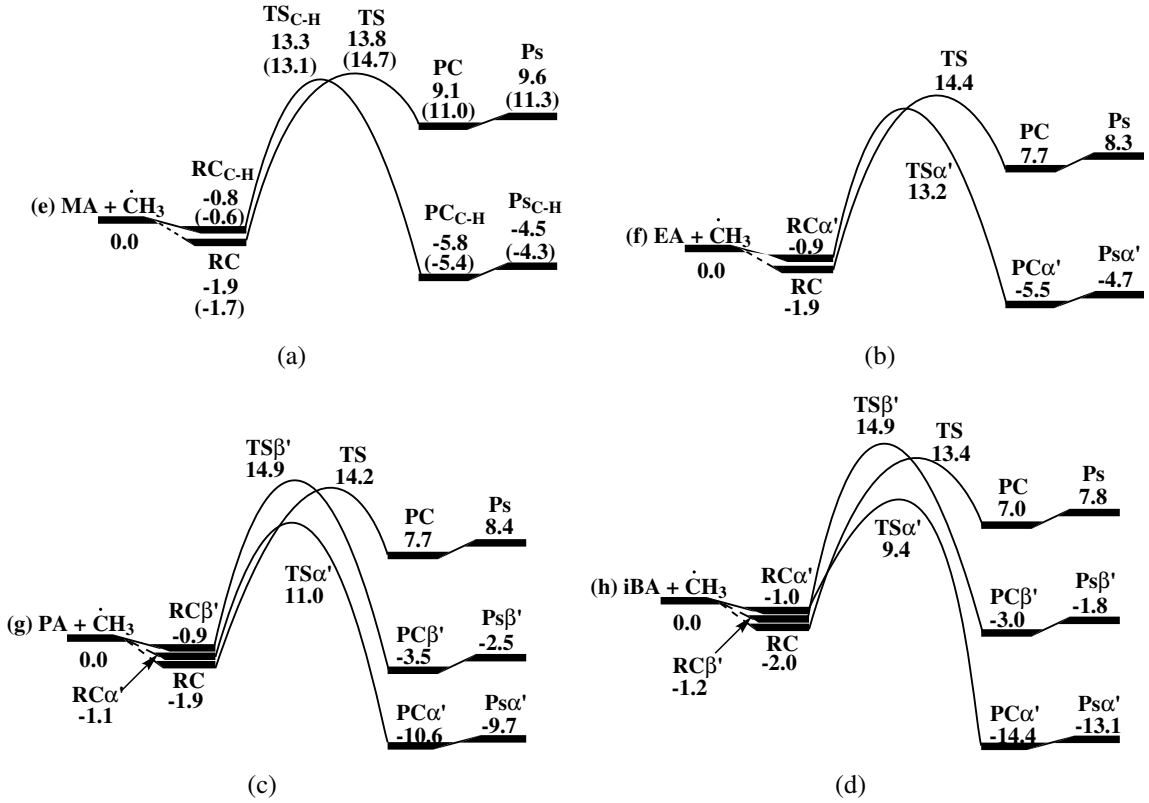

Figure 10: PES of the reactions of acids with $\dot{C}H_3$ radicals calculated with the CCSD(T)/cc-pVTZ and CCSD(T)/CBS (in parentheses) methods for (a) methanoic acid and calculated with the CCSD(T)/cc-pVTZ method for (b) ethanoic acid, (c) propanoic acid and (d) isobutanoic acid, in kcal mol^{-1}.

Table 2: Calculated electronic energies (in kcal mol^{-1}) of the transition states relative to the reactants for aldehydes and acids + $\dot{O}H$ radicals in this work, detailing the different types of hydrogen atoms present.

	Species		β'	α'		R′CO–H
(a)	Methanal	CH_2O				−0.4
(b)	Ethanal	CH_3CHO		3.3 (1°)		−2.3
(c)	Propanal	CH_3CH_2CHO	1.5 (1°)	2.4 (2°)		−2.5
(d)	Isobutanal	$(CH_3)_2CHCHO$	1.4 (1°)	0.2 (3°)		−3.2
					H–C(=O)OH	R′C(=O)O–H
(e)	Methanoic acid (MA)	HC(=O)OH			3.6	3.0
(f)	Ethanoic acid (EA)	$CH_3C(=O)OH$		4.2 (1°)		3.4
(g)	Propanoic acid (PA)	$CH_3CH_2C(=O)OH$	1.4 (1°)	1.6 (2°)		3.1
(h)	Isobutanoic acid (iBA)	$(CH_3)_2CHC(=O)OH$	1.4 (1°)	−0.3 (3°)		2.1

Table 3: Calculated electronic energies (in kcal mol^{-1}) of the transition states relative to the reactants for aldehydes and acids + $H\dot{O}_2$ radicals in this work, detailing the different types of hydrogen atoms present.

	Species		β'	α'		R′CO–H
(a)	Methanal	CH_2O				14.4
(b)	Ethanal	CH_3CHO		22.1 (1°)		12.4
(c)	Propanal	CH_3CH_2CHO	19.3 (1°)	18.3 (2°)		11.9
(d)	Isobutanal	$(CH_3)_2CHCHO$	19.3 (1°)	15.3 (3°)		11.0
					H–C(=O)OH	R′C(=O)O–H
(e)	Methanoic acid (MA)	HC(=O)OH			20.2	25.6
(f)	Ethanoic acid (EA)	$CH_3C(=O)OH$		20.9 (1°)		24.9
(g)	Propanoic acid (PA)	$CH_3CH_2C(=O)OH$	19.1 (1°)	17.4 (2°)		24.7
(h)	Isobutanoic acid (iBA)	$(CH_3)_2CHC(=O)OH$	19.0 (1°)	14.7 (3°)		23.6

Table 4: Calculated electronic energies (in kcal mol^{-1}) of the transition states relative to the reactants for aldehydes and acids + $\dot{C}H_3$ radicals in this work, detailing the different types of hydrogen atoms present.

	Species		β'	α'		R′CO–H
(a)	Methanal	CH_2O				11.1
(b)	Ethanal	CH_3CHO		14.0 (1°)		9.8
(c)	Propanal	CH_3CH_2CHO	14.9 (1°)	11.7 (2°)		9.5
(d)	Isobutanal	$(CH_3)_2CHCHO$	15.0 (1°)	9.7 (3°)		9.2
					H–C(=O)OH	R′C(=O)O–H
(e)	Methanoic acid (MA)	HC(=O)OH			13.3	13.8
(f)	Ethanoic acid (EA)	$CH_3C(=O)OH$		13.2 (1°)		14.4
(g)	Propanoic acid (PA)	$CH_3CH_2C(=O)OH$	14.9 (1°)	11.0 (2°)		14.2
(h)	Isobutanoic acid (iBA)	$(CH_3)_2CHC(=O)OH$	14.9 (1°)	9.4 (3°)		13.4

Rate Constant Calculations

The high-pressure limit rate constants have been calculated, in the temperature range from 500 to 2000 K, using the conventional transition state theory with an asymmetric Eckart tunneling

correction, as implemented in Variflex.[18] As in our previous studies,[3–8,10,11] herein we also use the one dimensional hindered rotor treatment in the determination of our rate constant results and the Pitzer–Gwinn-like approximation in order to fit the low-frequency torsional modes according to the following equation:

$$V = V_0 + \sum (V_n \times \cos n\theta) + \sum (V_m \times \sin m\theta)$$

Each dihedral angle of each reactant and transition state is investigated using the 1-D hindered rotor treatment and fitted using the equation above. Figure 11 shows an example of a potential energy diagram for an internal rotor and corresponding fit.

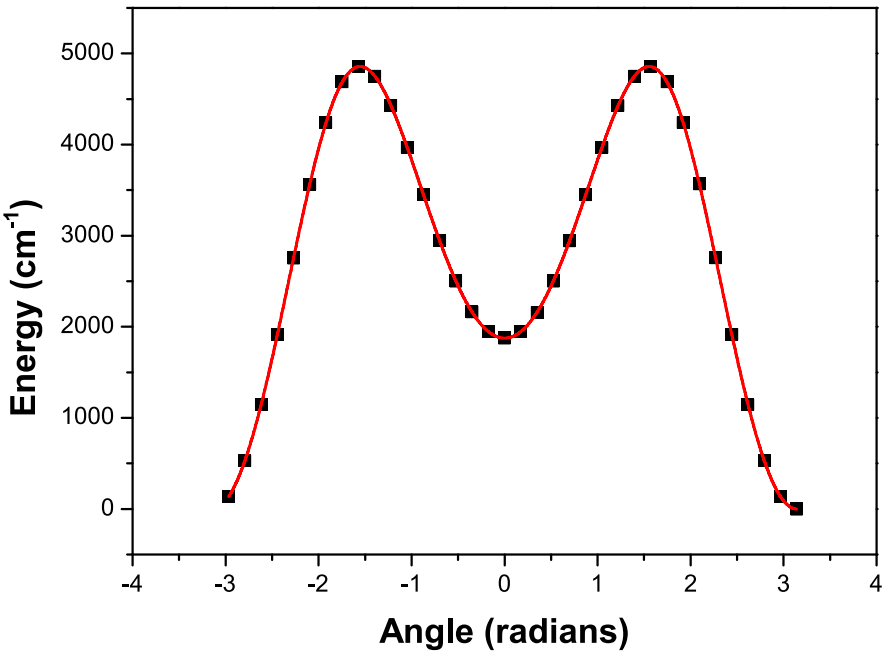

Figure 11: Potential energy diagram and fit for the internal rotation of the HC(=O)**–OH** dihedral angle in methanoic acid reactant.

We also provide Figure S1 in the SI which shows the hindered rotors fits for the H-atom abstraction reactions by $H\dot{O}_2$ radicals from isobutanoic acid.

Previously, when we compared our calculated results obtained using the one dimensional treatment[4] to those calculated by Truhlar and co-workers[19,20] with the multi-structure method, we observed that the results were quite similar and within 20 to 40% of one another.[10]

In our previous works,[8,21] we have studied the addition and H-atom abstraction reactions of ketones + $H\dot{O}_2$ radicals and we found that in the temperature range studied (600–1600 K) the H-atom abstraction reactions are faster than the addition reactions by more than 2 orders of magnitude. D'Anna *et al.*[22] have also studied the addition reaction of an $\dot{O}H$ radical to aldehydes and have found that these are of no importance under atmospheric conditions or even at the combustion temperature of 1500 K. Therefore, herein we disregard the addition of a radical to the carbonyl group of aldehydes and acids and only study the H-atom abstraction reactions.

Figures 12–14 show our calculated rate constants, on a per H-atom basis, for the aldehydes (solid lines) and acids (dashed lines) when reacting with $\dot{H}$ atoms (Figures 12(a), 13(a) and 14(a)), $\dot{O}H$ radicals ((Figures 12(b), 13(b) and 14(b))), $H\dot{O}_2$ radicals ((Figures 12(c), 13(c) and 14(c))) and $\dot{C}H_3$ radicals ((Figures 12(d), 13(d) and 14(d))). Figures 13(b) and 14(b) and Figures 13(c) and 14(c) also show a comparison with our previous calculated rate constants, on a per H-atom basis, for the abstraction of a hydrogen atom from esters (dashed dotted lines) by $\dot{O}H$[10] and $H\dot{O}_2$ radicals,[11] respectively.

Figures 12(a)–12(d) show our calculated rate constants for abstraction of the aldehylic hydrogen atom in aldehydes, the acidic hydrogen atom in acids and the H–C(=O)OH hydrogen atom in methanoic acid by $\dot{H}$ atoms and $\dot{O}H$, $H\dot{O}_2$ and $\dot{C}H_3$ radicals, respectively. We observe that abstracting the acidic hydrogen atom in acids, by any of the radicals studied, is slower than abstracting the aldehylic hydrogen atom of aldehydes throughout the whole temperature range. Abstracting the H–C(=O)OH hydrogen atom in methanoic acid is also slower than aldehydes; however, it is faster than abstracting the acidic hydrogen atom in acids, from 500–2000 K. This is due to the lower energy required to abstract an aldehylic hydrogen atom when compared to the energy required to abstract the acidic hydrogen atom in acids and the H–C(=O)OH hydrogen atom in methanoic acid.

Figures 13 and 14 show our calculated rate constants for abstracting a hydrogen atom at the α' and β' positions of aldehydes and acids, respectively. Abstraction of a hydrogen atom by any of the radicals studied at these positions in aldehydes is similar to abstracting the same type of hydrogen atom at the same position in acids. We also observed the same similarity when comparing to abstraction of the same type of hydrogen atom at the same position in esters, by an $\dot{O}H$ (Figures 13(b) and 14(b)) or $H\dot{O}_2$ radical (Figures 13(c) and 14(c)).

Figures 15(a)–15(d) show a comparison of the rate constants calculated in this work for aldehydes (Figures 15(a) and 15(b)) and acids (Figures 15(c) and 15(d)) with those calculated for alkanes, when reacting with an $\dot{O}H$[23] and $H\dot{O}_2$[24] radical, respectively. When reacting with $\dot{O}H$ radicals, abstraction of the aldehylic hydrogen atom from aldehydes is almost 3 orders of magnitude faster than alkanes[23] at 500 K, decreasing to a factor of 23 faster at 2000 K (Figure 15(a)). However, when abstracting the acidic hydrogen atom of the acids (Figure 15(c)), it is slower than alkanes[23] by about a factor of 2 to 4, from 500–2000 K, and it is similar to abstracting a hydrogen atom at the α' or β' positions. This is due to the oxygen atom in the functional group of the aldehydes donating the lone pair of electrons to the anti-bonding orbital of the adjacent C–H bond, weakening it. This decreases the energy required to abstract the hydrogen atom and, consequently, accelerates the rate constants. However, the -O–H bond in acids is strong which increases the energy required to abstract the hydrogen atom, decreasing the rate constants.

When undergoing abstraction by an $H\dot{O}_2$ radical, a similar trend is observed where abstracting an aldehylic hydrogen atom is faster than alkanes[24] by about 4.5 orders of magnitude at 500 K, decreasing to about an order of magnitude at 2000 K, Figure 15(b). Abstracting the acidic hydrogen atom in acids is slower than alkanes[24] by almost 2.5 orders of magnitude at 500 K, decreasing to about an order of magnitude at 2000 K, Figure 15(d). As with $\dot{O}H$ radicals, abstracting a hydrogen atom by $H\dot{O}_2$ radicals at the α' or β' positions of aldehydes and acids is also slower throughout the whole temperature range. At 1000 K, abstracting a hydrogen atom at those positions in aldehydes are in the range from 1–1.2 orders of magnitude slower than alkanes[24] and in acids they are in the range from 0.5–1 order of magnitude slower than alkanes.[24]

Tables 5–9 show the fit parameters of our rate constant results. Tables 5 and 6 and Tables 7 and 8 show the Arrhenius fit parameters for our individual and average rate constant results, respectively, on a per hydrogen atom basis. Table 9 shows the Arrhenius fit parameters for our total rate constants, for each aldehyde and acid studied.

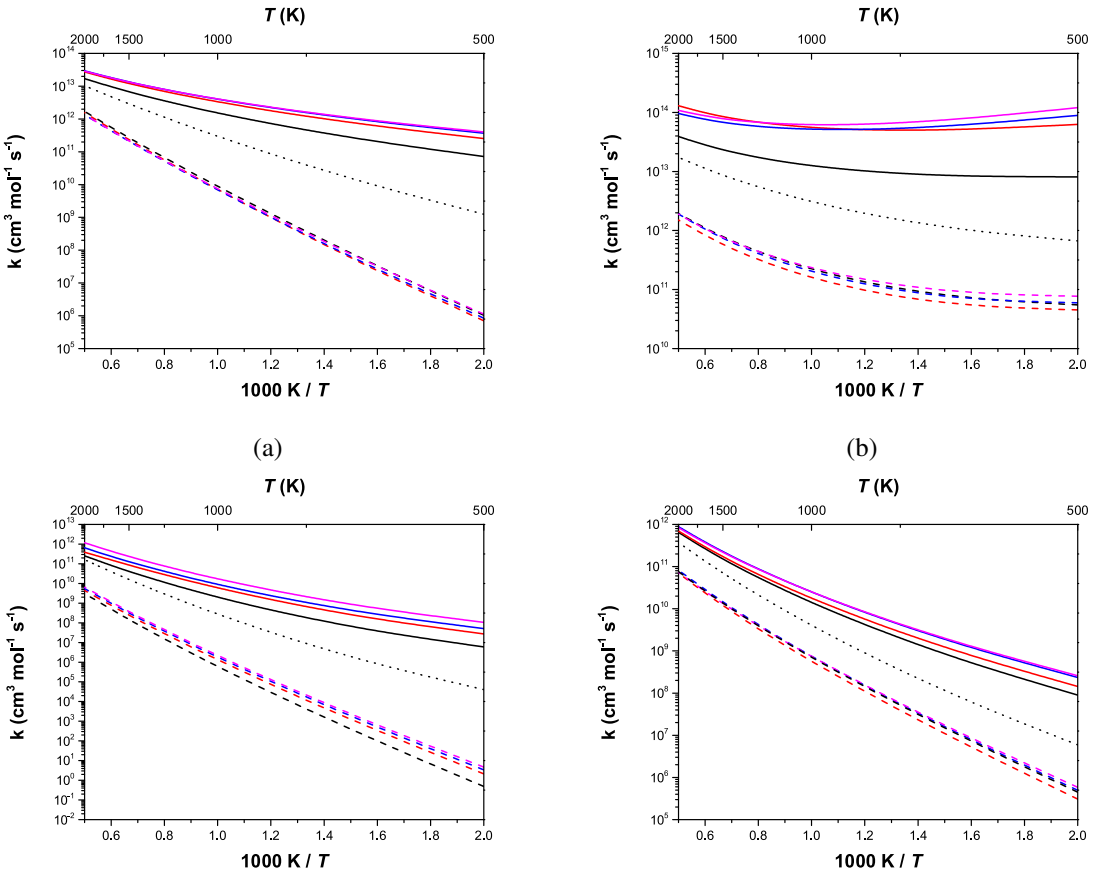

Figure 12: Rate constants comparison for abstraction of a hydrogen atom at the R′C(=O)–H/R′C(=O)O–H position, in cm^3 mol^{-1} s^{-1}. (a) abstraction by Ḣ atoms; (b) abstraction by ȮH radicals; (c) abstraction by $HȮ_2$ radicals; (d) abstraction by $ĊH_3$ radicals. Solid lines: aldehydes (methanal, black; ethanal, red; propanal, blue; isobutanal, magenta). Dashed lines: acids (methanoic acid, black; ethanoic acid, red; propanoic acid, blue; isobutanoic acid, magenta). Dotted line: abstraction of H–C(=O)OH.

Figure 16 shows our total rate constants for the reactions of methanal with Ḣ atoms (Figure 16(a)) and ȮH (Figure 16(b)), $HȮ_2$ (Figure 16(c)) and $ĊH_3$ (Figure 16(d)) radicals and a comparison to available experimental and theoretical data. Figure 17 shows our rate constants for the reactions of ethanal with Ḣ atoms (Figure 17(a)) and $HȮ_2$ radicals (Figure 17(d)) and ethanoic

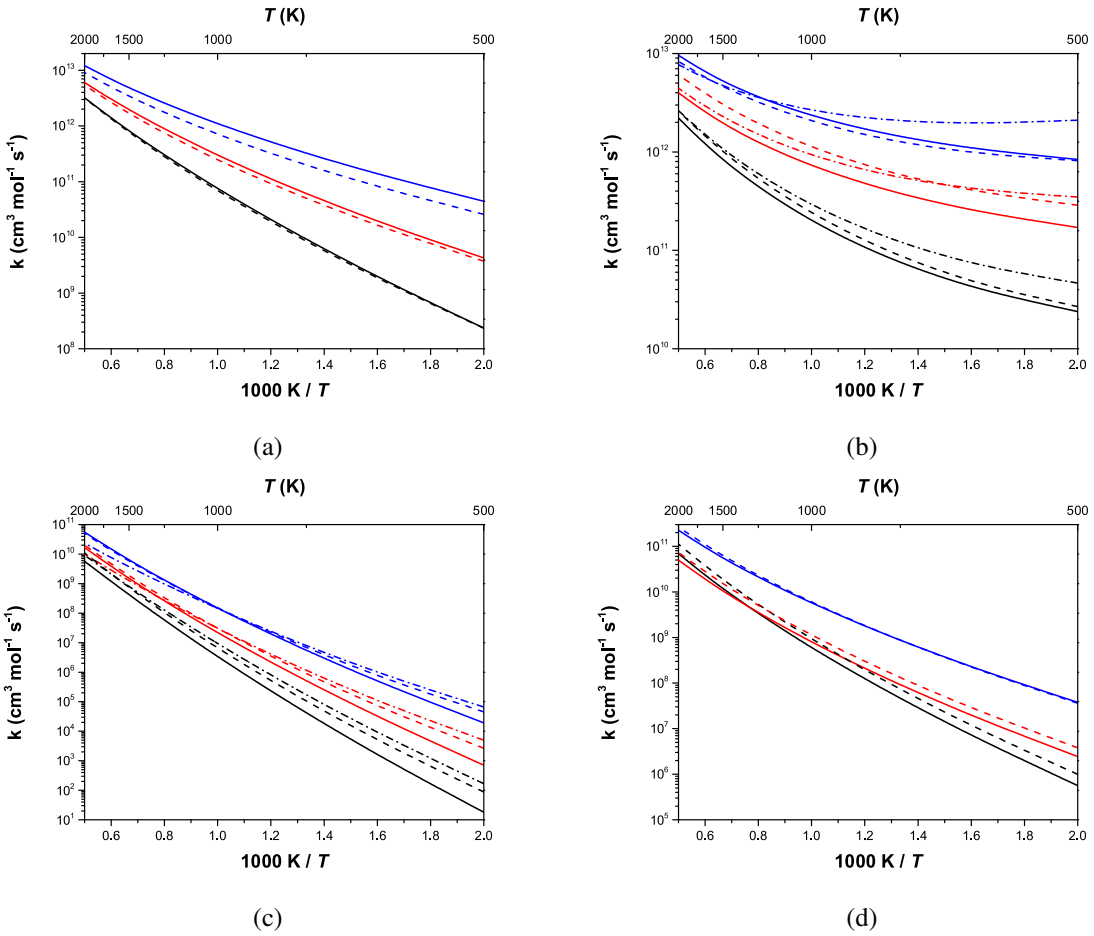

Figure 13: Rate constants comparison for abstraction of a hydrogen atom at the α' position, in cm^3 mol^{-1} s^{-1}. (a) abstraction by $\dot{H}$ atoms; (b) abstraction by $\dot{O}H$ radicals; (c) abstraction by $H\dot{O}_2$ radicals; (d) abstraction by $\dot{C}H_3$ radicals. Solid lines: aldehydes (ethanal, black; propanal, red; isobutanal, blue). Dashed lines: acids (ethanoic acid, black; propanoic acid, red; isobutanoic acid, blue). Dashed dotted line: (b) esters + $\dot{O}H$;[10] (c) esters + $H\dot{O}_2$.[11]

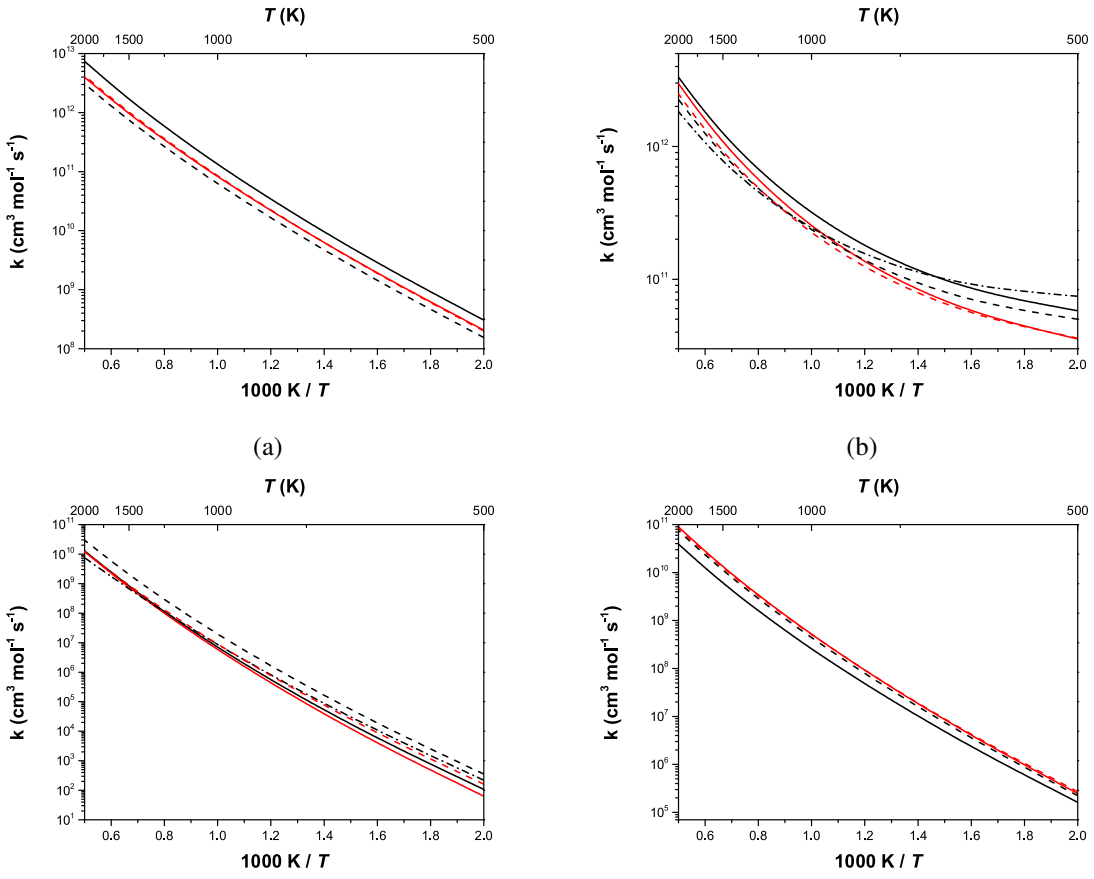

Figure 14: Rate constants comparison for abstraction of a hydrogen atom at the β' position, in cm^3 mol^{-1} s^{-1}. (a) abstraction by $\dot{H}$ atoms; (b) abstraction by $\dot{O}H$ radicals; (c) abstraction by $H\dot{O}_2$ radicals; (d) abstraction by $\dot{C}H_3$ radicals. Solid lines: aldehydes (propanal, black; isobutanal, red). Dashed lines: acids (propanoic acid, black; isobutanoic acid, red). Dashed dotted line: (b) esters + $\dot{O}H$;[10] (c) esters + $H\dot{O}_2$.[11]

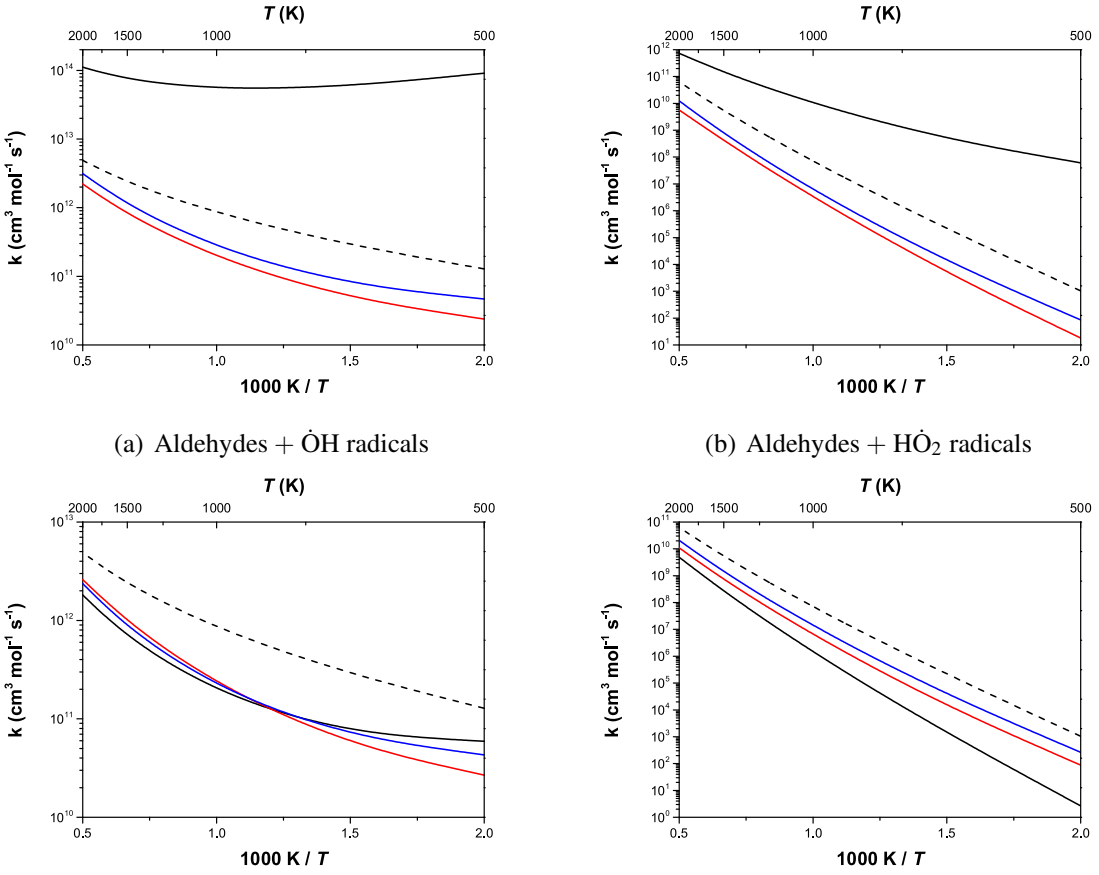

(a) Aldehydes + $\dot{O}H$ radicals

(b) Aldehydes + $H\dot{O}_2$ radicals

(c) Acids + $\dot{O}H$ radicals

(d) Acids + $H\dot{O}_2$ radicals

Figure 15: Rate constants comparison for abstraction of a primary hydrogen atom at each position of aldehydes and acids, in $cm^3\ mol^{-1}\ s^{-1}$. Aldehydes (– R′C(=O)–H, – α', – β') + (a) $\dot{O}H$ (– – alkanes[23]), (b) $H\dot{O}_2$ (– – alkanes[24]); acids (– R′C(=O)O–H, – α', – β') + (c) $\dot{O}H$ (– – alkanes[23]), (d) $H\dot{O}_2$ (– – alkanes[24]).

Table 5: Rate constants Arrhenius fit parameters (A, n and E), in cm^3 mol^{-1} s^{-1}, at each position of the acids and aldehydes, when reacting with Ḣ atoms and ȮH radicals in this work, on a per hydrogen atom basis.

	Position	H-Atom Type	Species	A	n	E
+ Ḣ atoms	R′C(=O)–**H**		Methanal	$9.46 \times 10^{+4}$	2.6	2569.
			Ethanal	$6.90 \times 10^{+5}$	2.4	1905.
			Propanal	$8.46 \times 10^{+5}$	2.3	1545.
			Isobutanal	$8.66 \times 10^{+5}$	2.3	1426.
	R′C(=O)O–**H**		Methanoic acid (MA)	$7.09 \times 10^{+6}$	2.1	15115.
			Ethanoic acid (EA)	$1.79 \times 10^{+6}$	2.3	15215.
			Propanoic acid (PA)	$1.62 \times 10^{+6}$	2.3	14796.
			Isobutanoic acid (iBA)	$7.41 \times 10^{+5}$	2.4	14252.
	H–C(=O)OH		Methanoic acid (MA)	$7.46 \times 10^{+5}$	2.4	7643.
	α'	1°	Ethanal	$1.05 \times 10^{+5}$	2.5	8041.
		2°	Propanal	$7.89 \times 10^{+4}$	2.6	4993.
		3°	Isobutanal	$6.08 \times 10^{+5}$	2.3	3220.
		1°	Ethanoic acid (EA)	$5.61 \times 10^{+3}$	2.9	7376.
		2°	Propanoic acid (PA)	$4.47 \times 10^{+3}$	2.9	4402.
		3°	Isobutanoic acid (iBA)	$5.04 \times 10^{+4}$	2.6	3048.
	β'	1°	Propanal	$1.80 \times 10^{+4}$	2.9	8157.
		1°	Isobutanal	$9.89 \times 10^{+4}$	2.6	8382.
		1°	Propanoic acid (PA)	$5.52 \times 10^{+4}$	2.6	8360.
		1°	Isobutanoic acid (iBA)	$1.04 \times 10^{+5}$	2.6	8512.
+ ȮH radicals	R′C(=O)–**H**		Methanal	$2.81 \times 10^{+4}$	2.7	−2808.
			Ethanal	$1.12 \times 10^{+5}$	2.6	−3835.
			Propanal	$1.06 \times 10^{+5}$	2.6	−4597.
			Isobutanal	$9.44 \times 10^{+4}$	2.6	−4873.
	R′C(=O)O–**H**		Methanoic acid (MA)	4.66×10^{-3}	4.3	−3095.
			Ethanoic acid (EA)	1.06×10^{-4}	4.8	−3949.
			Propanoic acid (PA)	1.18×10^{-4}	4.8	−4029.
			Isobutanoic acid (iBA)	8.39×10^{-4}	4.5	−3943.
	H–C(=O)OH		Methanoic acid (MA)	$6.32 \times 10^{+3}$	2.8	−789.
	α'	1°	Ethanal	2.02×10^{-1}	3.9	−1068.
		2°	Propanal	$1.47 \times 10^{+3}$	2.8	−973.
		3°	Isobutanal	$1.98 \times 10^{+4}$	2.6	−1488.
		1°	Ethanoic acid (EA)	7.34×10^{-1}	3.8	−725.
		2°	Propanoic acid (PA)	$9.34 \times 10^{+2}$	2.9	−1260.
		3°	Isobutanoic acid (iBA)	$5.57 \times 10^{+3}$	2.7	−1843.
	β'	1°	Propanal	4.51×10^{-3}	4.4	−2615.
		1°	Isobutanal	5.89×10^{-3}	4.4	−2054.
		1°	Propanoic acid (PA)	4.30×10^{-3}	4.4	−2859.
		1°	Isobutanoic acid (iBA)	4.30×10^{-3}	4.4	−2332.

$k = A \times T^n \times \exp(-E/RT)$, where R = 1.987 cal K^{-1} mol^{-1}

Table 6: Rate constants Arrhenius fit parameters (A, n and E), in $cm^3\ mol^{-1}\ s^{-1}$, at each position of the acids and aldehydes, when reacting with $H\dot{O}_2$ and $\dot{C}H_3$ radicals in this work, on a per hydrogen atom basis.

	Position	H-Atom Type	Species	A	n	E
$+ H\dot{O}_2$ radicals	R′C(=O)–**H**		Methanal	7.76×10^{-8}	5.8	3870.
			Ethanal	2.78×10^{-3}	4.5	4829.
			Propanal	3.72×10^{-5}	5.0	3504.
			Isobutanal	1.01×10^{-4}	5.0	3429.
	R′C(=O)O–**H**		Methanoic acid	1.66×10^{-3}	4.4	21866.
			Ethanoic acid	1.41×10^{-2}	4.2	20862.
			Propanoic acid	1.86×10^{-2}	4.2	20585.
			Isobutanoic acid	8.03×10^{-3}	4.3	20170.
	H–C(=O)OH		Methanoic acid	9.72×10^{-8}	5.9	9759.
	α'	1°	Ethanal	1.81×10^{-2}	4.1	18648.
		2°	Propanal	3.42×10^{-3}	4.3	14694.
		3°	Isobutanal	8.19×10^{-3}	4.3	11994.
		1°	Ethanoic acid	1.34×10^{-6}	5.3	15153.
		2°	Propanoic acid	5.16×10^{-7}	5.4	11311.
		3°	Isobutanoic acid	5.37×10^{-6}	5.2	9206.
	β'	1°	Propanal	1.87×10^{-8}	5.9	14091.
		1°	Isobutanal	9.58×10^{-8}	5.7	15070.
		1°	Propanoic acid	8.37×10^{-7}	5.5	14219.
		1°	Isobutanoic acid	3.01×10^{-6}	5.2	14642.
$+ \dot{C}H_3$ radicals	R′C(=O)–**H**		Methanal	5.74×10^{-1}	3.8	4873.
			Ethanal	$1.55 \times 10^{+0}$	3.7	4564.
			Propanal	$2.99 \times 10^{+0}$	3.6	4338.
			Isobutanal	$3.94 \times 10^{+0}$	3.6	4223.
	R′C(=O)O–**H**		Methanoic acid	$2.96 \times 10^{+2}$	2.9	10637.
			Ethanoic acid	$9.30 \times 10^{+1}$	3.0	10773.
			Propanoic acid	$1.32 \times 10^{+2}$	3.0	10421.
			Isobutanoic acid	$1.84 \times 10^{+2}$	2.9	10167.
	H–C(=O)OH		Methanoic acid (MA)	$1.59 \times 10^{+0}$	3.7	7963.
	α'	1°	Ethanal	4.79×10^{-1}	3.7	8857.
		2°	Propanal	3.08×10^{-1}	3.6	6581.
		3°	Isobutanal	$5.90 \times 10^{+0}$	3.4	5351.
		1°	Ethanoic acid	7.13×10^{-2}	4.0	8222.
		2°	Propanoic acid	5.91×10^{-2}	3.9	6066.
		3°	Isobutanoic acid	$1.42 \times 10^{+0}$	3.6	5264.
	β'	1°	Propanal	3.49×10^{-2}	4.0	9253.
		1°	Isobutanal	1.33×10^{-1}	3.9	9882.
		1°	Propanoic acid	7.52×10^{-2}	4.0	9691.
		1°	Isobutanoic acid	1.37×10^{-1}	3.9	9694.

$k = A \times T^n \times \exp(-E/RT)$, where $R = 1.987$ cal K^{-1} mol^{-1}

Table 7: Average Arrhenius fit parameters (A, n and E), on a per-hydrogen atom basis according to hydrogen atom type (1°, 2° or 3°) and position (H–C(=O)OH, R′C(=O)O–H, R′C(=O)–H, α' and β') relative to the functional group of the aldehydes and acids, when reacting with Ḣ atoms and ȮH radicals in this work. Values in units of $cm^3\ mol^{-1}\ s^{-1}$.

	Position	H-Atom Type	Species	A	n	E
+ Ḣ atoms	**H**–C(=O)OH		Methanoic acid	$7.46 \times 10^{+5}$	2.4	7643.
	HC(=O)–**H**		Methanal	$9.46 \times 10^{+4}$	2.6	2569.
	R′C(=O)–**H**		Aldehydes	$7.15 \times 10^{+5}$	2.4	1577.
	R′C(=O)O–**H**		Acids	$1.72 \times 10^{+6}$	2.3	14799.
	α'	1°		$1.05 \times 10^{+5}$	2.5	8041.
		2°	Aldehydes	$7.89 \times 10^{+4}$	2.6	4993.
		3°		$6.08 \times 10^{+5}$	2.3	3220.
		1°		$5.61 \times 10^{+3}$	2.9	7376.
		2°	Acids	$4.47 \times 10^{+3}$	2.9	4402.
		3°		$5.04 \times 10^{+4}$	2.6	3047.
	β'	1°	Aldehydes	$3.17 \times 10^{+4}$	2.8	8230.
		1°	Acids	$7.81 \times 10^{+4}$	2.6	8446.
+ ȮH radicals	**H**–C(=O)OH		Methanoic acid	$6.32 \times 10^{+3}$	2.8	−789.
	HC(=O)–**H**		Methanal	$2.81 \times 10^{+4}$	2.7	−2808.
	R′C(=O)–**H**		Aldehydes	$6.13 \times 10^{+4}$	2.7	−4586.
	R′C(=O)O–**H**		Acids	4.84×10^{-4}	4.6	−3766.
	α'	1°		2.02×10^{-1}	3.9	−1068.
		2°	Aldehydes	$1.47 \times 10^{+3}$	2.8	−973.
		3°		$1.98 \times 10^{+4}$	2.6	−1488.
		1°		7.34×10^{-1}	3.8	−725.
		2°	Acids	$9.34 \times 10^{+2}$	2.9	−1260.
		3°		$5.57 \times 10^{+3}$	2.7	−1843.
	β'	1°	Aldehydes	4.36×10^{-3}	4.4	−2406.
		1°	Acids	3.58×10^{-3}	4.4	−2652.

$k = A \times T^n \times \exp(-E/RT)$, where $R = 1.987$ cal K^{-1} mol^{-1}

Table 8: Average Arrhenius fit parameters (A, n and E), on a per-hydrogen atom basis according to hydrogen atom type (1°, 2° or 3°) and position (H–C(=O)OH, R′C(=O)O–H, R′C(=O)–H, α' and β') relative to the functional group of the aldehydes and acids, when reacting with $H\dot{O}_2$ and $\dot{C}H_3$ radicals in this work. Values in units of $cm^3\ mol^{-1}\ s^{-1}$.

	Position	H-Atom Type	Species	A	n	E
+ $H\dot{O}_2$ radicals	**H**–C(=O)OH		Methanoic acid	9.72×10^{-8}	5.9	9759.
	HC(=O)–**H**		Methanal	7.76×10^{-8}	5.8	3870.
	R′C(=O)–**H**		Aldehydes	1.18×10^{-4}	4.9	3684.
	R′C(=O)O–**H**		Acids	4.46×10^{-3}	4.3	20436.
	α'	1°	Aldehydes	1.81×10^{-2}	4.1	18648.
		2°		3.42×10^{-3}	4.3	14694.
		3°		8.19×10^{-3}	4.3	11994.
		1°	Acids	1.34×10^{-6}	5.3	15153.
		2°		5.16×10^{-7}	5.4	11311.
		3°		5.37×10^{-6}	5.2	9206.
	β'	1°	Aldehydes	3.09×10^{-8}	5.8	14468.
		1°	Acids	1.14×10^{-6}	5.4	14348.
+ $\dot{C}H_3$ radicals	**H**–C(=O)OH		Methanoic acid	$1.59 \times 10^{+0}$	3.7	7963.
	HC(=O)–**H**		Methanal	5.74×10^{-1}	3.8	4873.
	R′C(=O)–**H**		Aldehydes	$2.50 \times 10^{+0}$	3.6	4329.
	R′C(=O)O–**H**		Acids	$1.39 \times 10^{+2}$	3.0	10436.
	α'	1°	Aldehydes	4.79×10^{-1}	3.7	8857.
		2°		3.08×10^{-1}	3.6	6581.
		3°		$5.90 \times 10^{+0}$	3.4	5351.
		1°	Acids	7.13×10^{-2}	4.0	8222.
		2°		5.91×10^{-2}	3.9	6066.
		3°		$1.42 \times 10^{+0}$	3.6	5264.
	β'	1°	Aldehydes	6.85×10^{-2}	4.0	9629.
		1°	Acids	1.03×10^{-1}	3.9	9691.

$k = A \times T^n \times \exp(-E/RT)$, where $R = 1.987$ cal K^{-1} mol^{-1}

Table 9: Arrhenius fit parameters for the total rate constants in this work. Values in units of cm^3 mol^{-1} s^{-1}.

	Species	A	n	E
+ Ḣ atoms	Methanal	$1.89 \times 10^{+5}$	2.6	2569.
	Ethanal	$9.38 \times 10^{+3}$	2.9	1215.
	Propanal	$7.19 \times 10^{+1}$	3.6	148.
	Isobutanal	$5.17 \times 10^{+2}$	3.4	410.
	MA	$7.88 \times 10^{+4}$	2.7	7274.
	EA	$1.99 \times 10^{+3}$	3.2	7039.
	PA	$1.30 \times 10^{+2}$	3.5	4081.
	iBA	3.32×10^{-1}	4.3	1737.
+ ȮH radicals	Methanal	$5.63 \times 10^{+4}$	2.7	−2808.
	Ethanal	$5.52 \times 10^{+4}$	2.7	−3950.
	Propanal	$1.19 \times 10^{+4}$	2.9	−4937.
	Isobutanal	$5.44 \times 10^{+3}$	3.0	−5320.
	MA	$2.71 \times 10^{+3}$	3.0	−973.
	EA	1.99×10^{-1}	4.1	−1627.
	PA	$4.57 \times 10^{+1}$	3.5	−1946.
	iBA	$1.70 \times 10^{+0}$	3.9	−2949.
+ $H\dot{O}_2$ radicals	Methanal	1.55×10^{-7}	5.8	3870.
	Ethanal	1.24×10^{-3}	4.6	4676.
	Propanal	5.46×10^{-6}	5.3	3148.
	Isobutanal	1.69×10^{-5}	5.2	3106.
	MA	7.03×10^{-8}	5.9	9702.
	EA	2.16×10^{-6}	5.4	15136.
	PA	1.13×10^{-8}	6.2	11288.
	iBA	1.43×10^{-10}	6.6	7771.
+ $\dot{C}H_3$ radicals	Methanal	$1.15 \times 10^{+0}$	3.8	4873.
	Ethanal	1.28×10^{-1}	4.0	4250.
	Propanal	4.46×10^{-1}	3.9	4097.
	Isobutanal	2.00×10^{-2}	4.3	3484.
	MA	$3.09 \times 10^{+0}$	3.7	8206.
	EA	6.47×10^{-1}	3.9	8543.
	PA	1.97×10^{-3}	4.6	6152.
	iBA	1.61×10^{-4}	4.9	4340.

$k = A \times T^n \times \exp(-E/RT)$, where R = 1.987 cal K^{-1} mol^{-1}

acid with $\dot{O}H$ radicals (Figure 17(e)), and corresponding comparison to available theoretical and experimental data.

Figure 16(a) shows our rate constants for methanal + $\dot{H}$ atoms and comparison to experimental data obtained by Friedrichs *et al.*[25] and our results are 67–90% slower.

In Figure 16(b) we compare our total rate constant results for methanal + $\dot{O}H$ radicals to experimental data obtained by Vasudevan *et al.*,[26] Wang *et al.*,[27] Vandooren *et al.*,[28] Westenberg *et al.*[29] and to theoretical results obtained by Li *et al.*,[30] D'Anna *et al.*[22] and Xu *et al.*[31] When comparing to experimental data obtained by Vasudevan *et al.*[26] and theoretical data obtained by Xu *et al.*,[31] our results predict accurately the temperature dependence of the rate constants but are about a factor of 2.5 faster throughout the studied temperature range. When we compare to more recent experimental data obtained by Wang *et al.*[27] our total rate constant results are a factor of 2 faster from 950–1400 K. This might be a combination of the error associated with the experimental data and the uncertainty in the theoretical results. When we compare to experimental data obtained by Vandooren *et al.*[28] and Westenberg *et al.*,[29] our results are in better agreement although the experimental data does not seem to predict accurately the temperature dependence of the rate constants. When comparing to theoretical calculations obtained by Li *et al.*[30] and D'Anna *et al.*[22] our results are within about $20-25\%$ above 1000 K. At 500 K D'Anna *et al.*[22] results are slower by about 65% while the results by Li *et al.*[30] are slower by about a factor of 5.

Figure 16(c) shows a comparison of our calculated results for methanal + $H\dot{O}_2$ radicals to theoretical results obtained by Li *et al.*,[32] Eiteneer *et al.*,[33] and to an estimated expression based on the works by Jemi-Alade *et al.*[34] and other low temperature measurements, as detailed by Robertson *et al.*[35] We observe that our results are within about a factor of 2 for most of the temperature range.

Figure 16(d) shows our rate constants for methanal + $\dot{C}H_3$ radicals and comparison to the experimental data obtained by Choudhury *et al.*[36] and theoretical calculations obtained by Li *et al.*[30] Our results are in good agreement with the experimental results[36] and are about a factor of 2 faster than the theoretical results.[30]

Figure 17(a) shows a comparison of our calculated rate constants for ethanal + $\dot{H}$ atoms to experimental data obtained by Bentz *et al.*[37] and our results are in good agreement with the experimental results.

Figure 17(b) shows a comparison of our calculated rate constants for ethanal + $\dot{O}H$ radicals to experimental data obtained by Wang *et al.*[27] and Taylor *et al.*[38] and to theoretical data by D'Anna *et al.*[22] and our results are faster than the experimental and theoretical results by about a factor of 5.

Figure 17(c) shows a comparison of our calculated rate constants for propanal + $\dot{O}H$ radicals to experimental data obtained by Wang *et al.*[27] and our results are faster than the experimental results by about a factor of 4.

Figure 17(d) shows our rate constants for abstraction of the aldehylic hydrogen atom of ethanal by $H\dot{O}_2$ radicals and a comparison to the theoretical results recommended by Farnia *et al.*[39] and da Silva *et al.*[40] Our results are in good agreement with the recommended results of da Silva *et al.*[40] and are about one order of magnitude slower than the results by Farnia *et al.*[39]

Figure 17(e) shows a comparison of our calculated rate constants for ethanoic acid + $\dot{O}H$ radicals to experimental data obtained by Khamaganov *et al.*[41] and our results are within about a factor of 2 of the experimental results.

A comparison of our calculated energies for methanal and ethanal + $\dot{O}H$ radicals and calculated frequencies for methanal + $\dot{O}H$ radicals to those calculated by Vasudevan *et al.*[26] and D'Anna *et al.*[22] is given in Table 10. It can be observed that the calculated energies and frequencies are very similar to one another but the calculated total rate constants differ. We do not know the reasons for these discrepancies as seen in Figures 16(b), 17(b) and 17(c); however, this work is based on systematic high-level *ab-initio* calculations which in previous works, such as in our work with esters + $\dot{O}H$ radicals,[10] have proven to give accurate results when compared to available experimental data.

Based on our previous work on *n*-butanol + $\dot{C}H_3$ radicals[42] and on the suggestion by Goldsmith *et al.*,[43] we have previously[6,11] estimated an overall uncertainty of a factor of 2.5. Herein, we

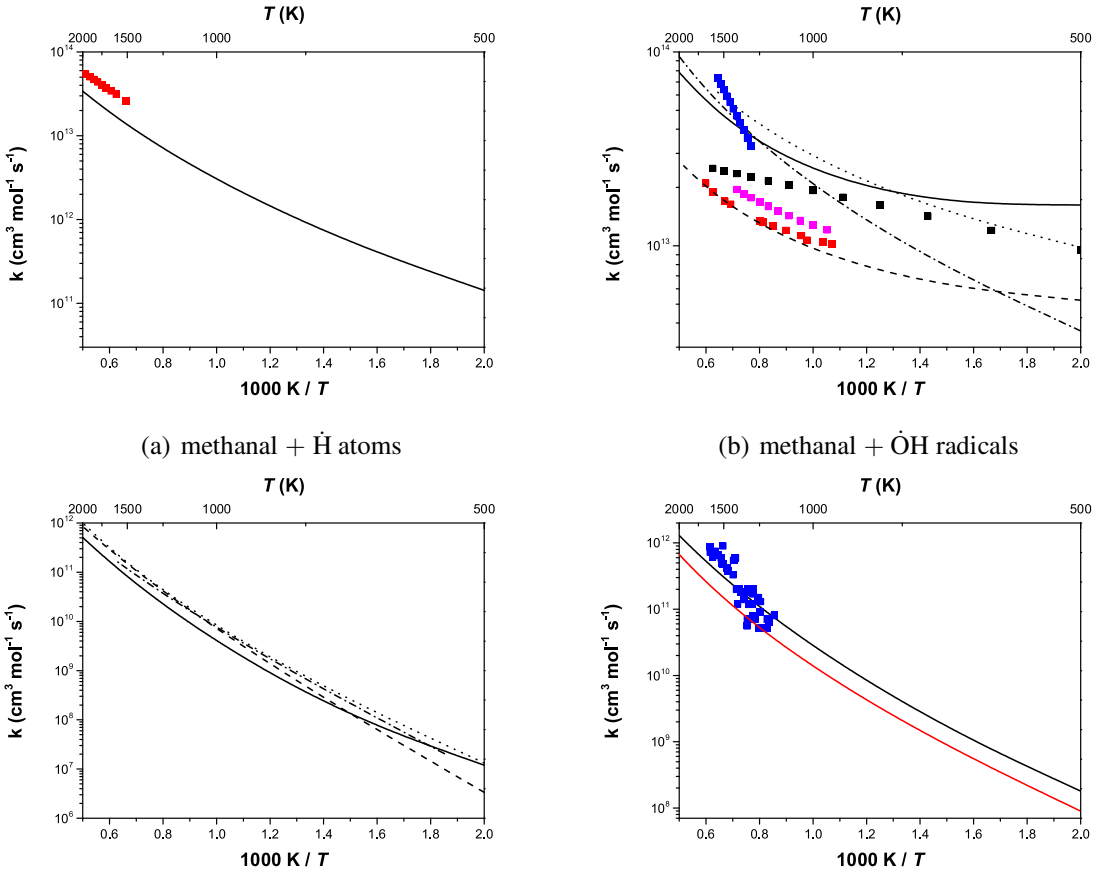

(a) methanal + Ḣ atoms

(b) methanal + ȮH radicals

(c) methanal + HȮ$_2$ radicals

(d) methanal + ĊH$_3$ radicals

Figure 16: Rate constants in this work for methanal + (a) Ḣ (b) ȮH, (c) HȮ$_2$ and (d) ĊH$_3$ radicals and comparison to available experimental and theoretical data. (a) – methanal + Ḣ, ■ Friedrichs *et al.*[25] (b) – methanal + ȮH, -.- Li *et al.*,[30] ... D'Anna *et al.*,[22] - - Xu *et al.*,[31] ■ Vasudevan *et al.*,[26] ■ Wang *et al.*,[27] ■ Vandooren *et al.*,[28] ■ Westenberg *et al.*[29] (c) – methanal + HȮ$_2$, - - Li *et al.*,[32] -.- Eiteneer *et al.*,[33] ... Robertson *et al.*[35] (d) – methanal + ĊH$_3$, ■ Choudhury *et al.*,[36] – Li *et al.*[30]

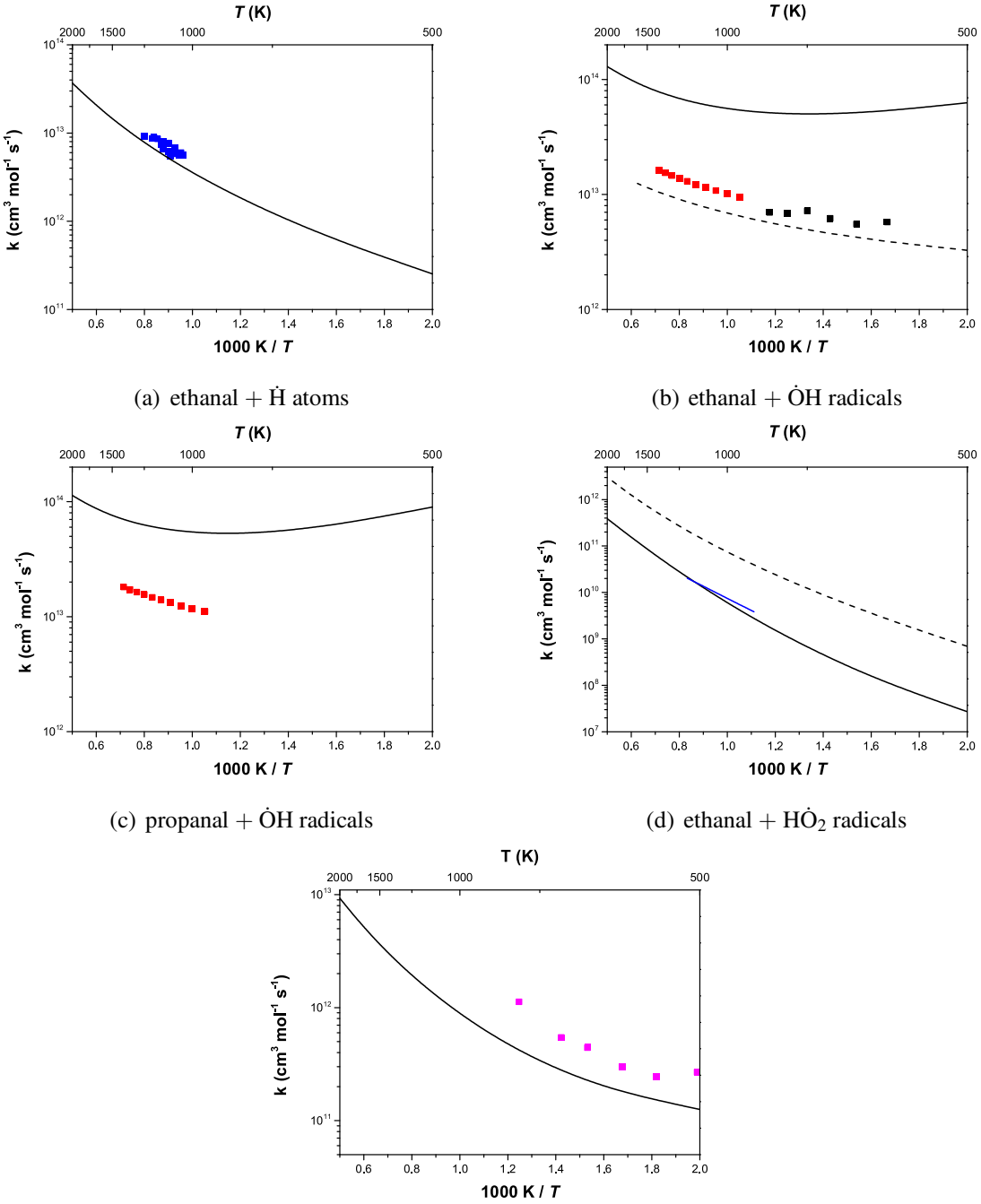

(a) ethanal + Ḣ atoms

(b) ethanal + ȮH radicals

(c) propanal + ȮH radicals

(d) ethanal + HȮ$_2$ radicals

(e) ethanoic acid + ȮH radicals

Figure 17: Rate constants in this work for ethanal + (a) Ḣ atoms, (b) HȮ$_2$ radicals and (c) ethanoic acid + ȮH radicals and comparison to available experimental and theoretical data. (a) – ethanal + Ḣ, ■ Bentz *et al.*[37] (b) – ethanal + ȮH, ■ Wang *et al.*,[27] ■ Taylor *et al.*,[38] - - D'Anna *et al.*[22] (c) – propanal + ȮH, ■ Wang *et al.*[27] (d) – ethanal + HȮ$_2$, - - Farnia *et al.*,[39] – da Silva *et al.*[40] (e) – ethanoic acid + ȮH, ■ Khamaganov *et al.*[41]

Table 10: Calculated relative electronic energies (in kcal mol^{-1}) and frequencies of the transition states for methanal and ethanal + $\dot{O}H$ radicals in this work, and comparison to theoretical results by Vasudevan *et al.*[26] and D'Anna *et al.*[22] Frequencies corresponding to the torsional modes are shown in bold.

	Methanal + $\dot{O}H$		Ethanal + $\dot{O}H$
	Energies (kcal mol^{-1})	**Frequencies (cm^{-1})**	**Energies (kcal mol^{-1})**
This work	−0.4	1611*i*, 105, 148, **191**, 807, 909, 1255, 1357, 1563, 2245, 2965, 3840	−2.3
Vasudevan *et al.*[26]	0.22	774*i*, 116, 120, **189**, 731, 1152, 1209, 1246, 1536, 1868, 2969, 3792	
D'Anna *et al.*[22]	−0.7	1532*i*, 106, 112, 226, 771, 873, 1186, 1226, 1515, 2256, 2983, 3755	−2.3

perform a similar systematic study of the hydrogen atom abstraction by $\dot{H}$ atoms and $\dot{O}H$, $H\dot{O}_2$ and $\dot{C}H_3$ radicals on aldehydes and acids and we also estimate an uncertainty of a factor of 2.5.

Conclusions

Conventional transition state theory with an asymmetric Eckart tunneling correction has been used to calculate the high-pressure limit rate constants for the title reactions, in the temperature range from 500 to 2000 K. As in our previous works,[3–11] complexes have been found in the entrance and exit channels when aldehydes and acids react with $\dot{O}H$, $H\dot{O}_2$ and $\dot{C}H_3$ radicals. However, when reacting with $\dot{H}$ atoms the formation of the reactant complexes was not observed in the entrance channel where aldehydes and acids react directly with the radical via the transition state to undergo abstraction of a hydrogen atom. Our calculated results were compared to previous works on esters[10,11] and alkanes calculated by Sivaramakrishnan *et al.*[23] and Iparraguirre et al.[24]

When a hydrogen atom is abstracted by $\dot{O}H$ and $H\dot{O}_2$ radicals from the α' and β' positions of aldehydes and acids we observe a similar trend where our results are generally slower compared to alkanes for the whole temperature range and they are similar to our previous work on esters.[10,11]

Abstraction of an aldehylic hydrogen atom is faster than alkanes due to the delocalization of the lone pair of electrons from the oxygen atom of the functional group of aldehydes into the anti-bonding orbital of the adjacent C–H bond. This weakens the bond (BDE = 86–87 kcal mol^{-1}), lowering the energy required for abstraction of the hydrogen atom and consequently accelerating the rate constants. Abstracting the acidic hydrogen atom in acids however is slower than alkanes due to the higher strength of the bond (BDE = 110–112 kcal mol^{-1}) which increases the energy required to break the bond and slows the rate constants.

We have compared our theoretical calculations for the reactions of methanal with $\dot{H}$ atoms and $\dot{O}H$, $H\dot{O}_2$ and $\dot{C}H_3$ radicals, ethanal with $\dot{H}$ atoms and $\dot{O}H$ and $H\dot{O}_2$ radicals, propanal and ethanoic acid with $\dot{O}H$ radicals to experimental and theoretical data obtained previously and our results are generally in good agreement.

Acknowledgement

This work was supported by Science Foundation Ireland under grant number [08/IN1./I2055]. Computational resources were provided by the Irish Center for High-End Computing (ICHEC).

Supporting Information Available

Tables S1, S3, S5 and S7 of the Supplementary Information (SI) provide details of the CCSD(T)/cc-pVDZ (TZ, QZ) and CCSD(T)/CBS calculated relative electronic energies for the abstraction of a hydrogen atom by $\dot{H}$ atoms and $\dot{O}H$, $H\dot{O}_2$ and $\dot{C}H_3$ radicals, respectively, from methanal and methanoic acid. Tables S2, S4, S6 and S8 of the SI provides the geometry co-ordinates and frequencies for the reactants and transitions states in the title reactions. Figure S1 shows the hindered rotors fits for the H-atom abstraction reactions by $H\dot{O}_2$ radicals from isobutanoic acid.

This material is available free of charge via the Internet at `http://pubs.acs.org/`.

References

(1) Wang, S.; Davidson, D. F.; Hanson, R. K. High-Temperature Laser Absorption Diagnostics for CH_2O and CH_3CHO and their Application to Shock Tube Kinetic Studies. *Combust. Flame* **2013**, *160*, 1930–1938.

(2) Anglada, J. M. Complex Mechanism of the Gas Phase Reaction between Formic Acid and Hydroxyl Radical. Proton Coupled Electron Transfer versus Radical Hydrogen Abstraction Mechanisms. *J. Am. Chem. Soc.* **2004**, *126*, 9809–9820, PMID: 15291585.

(3) Zhou, C.-W.; Simmie, J. M.; Curran, H. J. Rate Constants For Hydrogen-Abstraction By $\dot{O}H$ From *n*-Butanol. *Combust. Flame* **2011**, *158*, 726–731, Special Issue on Kinetics.

(4) Zhou, C.-W.; Simmie, J. M.; Curran, H. J. Rate Constants For Hydrogen Abstraction By $H\dot{O}_2$ From *n*-Butanol. *Int. J. Chem. Kinet.* **2012**, *44*, 155–164.

(5) Zhou, C.-W.; Simmie, J. M.; Curran, H. J. An Ab Initio/Rice-Ramsperger-Kassel-Marcus Study Of The Hydrogen-Abstraction Reactions Of Methyl Ethers, $H_3COCH_{3-x}(CH_3)_x$, x = 0–2, By $\dot{O}H$; Mechanism And Kinetics. *Phys. Chem. Chem. Phys.* **2010**, *12*, 7221–7233.

(6) Mendes, J.; Zhou, C.-W.; Curran, H. J. Rate Constant Calculations Of H-Atom Abstraction Reactions From Ethers By $H\dot{O}_2$ Radicals. *J. Phys. Chem. A* **2014**, *118*, 1300–1308.

(7) Zhou, C.-W.; Simmie, J. M.; Curran, H. J. Ab Initio And Kinetic Study Of The Reaction Of Ketones With $\dot{O}H$ for T=500–2000 K. Part I: Hydrogen-Abstraction From $H_3CC(O)CH_{3-x}(CH_3)_x$, x = 0 $\rightarrow$ 2. *Phys. Chem. Chem. Phys.* **2011**, *13*, 11175–11192.

(8) Mendes, J.; Zhou, C.-W.; Curran, H. J. Theoretical And Kinetic Study Of The Reactions Of Ketones With $H\dot{O}_2$ Radicals. Part I: Abstraction Reaction Channels. *J. Phys. Chem. A* **2013**, *117*, 4515–4525.

(9) Mendes, J.; Zhou, C.-W.; Curran, H. J. Correction to Theoretical And Kinetic Study Of The

Reactions Of Ketones With $H\dot{O}_2$ Radicals. Part I: Abstraction Reaction Channels. *J. Phys. Chem. A* **2014**, *118*, 331–331.

(10) Mendes, J.; Zhou, C.-W.; Curran, H. J. Theoretical Study of the Rate Constants for the Hydrogen Atom Abstraction Reactions of Esters with $\dot{O}H$ Radicals. *J. Phys. Chem. A* **2014**, *118*, 4889–4899.

(11) Mendes, J.; Zhou, C.-W.; Curran, H. J. Theoretical And Kinetic Study Of The Hydrogen Atom Abstraction Reactions Of Esters With $H\dot{O}_2$ Radicals. *J. Phys. Chem. A* **2013**, *117*, 14006–14018.

(12) Frisch, M. J.; Trucks, G. W.; Schlegel, H. B.; Scuseria, G. E.; Robb, M. A.; Cheeseman, J. R.; Scalmani, G.; Barone, V.; Mennucci, B.; Petersson, G. A.; *et al.*, Gaussian 09 Revision A.1. Gaussian Inc. Wallingford CT 2009.

(13) Peterson, K. A.; Woon, D. E.; Dunning, T. H. Benchmark Calculations With Correlated Molecular Wave-Functions .4. The Classical Barrier Height Of The $H+H_2 \rightarrow H_2+H$ Reaction. *J. Chem. Phys.* **1994**, *100*, 7410–7415.

(14) Merrick, J. P.; Moran, D.; Radom, L. An Evaluation of Harmonic Vibrational Frequency Scale Factors. *J. Phys. Chem. A* **2007**, *111*, 11683–11700.

(15) ChemCraft v1.6 http://www.chemcraftprog.com/.

(16) Glasstone, S.; Laidler, K. J.; Eyring, H. Theory of Rate Processes. *McGraw-Hill: New York* **1941**,

(17) Eckart, C. The Penetration Of A Potential Barrier By Electrons. *Phys. Rev.* **1930**, *35*, 1303–1309.

(18) Klippenstein, S. J.; Wagner, A. F.; Dunbar, R. C.; Wardlaw, D. M.; Robertson, S. H. VariFlex, version 2.02m. Argonne National Laboratory, Argonne, IL, 1999.

(19) Alecu, I. M.; Zheng, J.; Papajak, E.; Yu, T.; Truhlar, D. G. Biofuel Combustion. Energetics And Kinetics Of Hydrogen Abstraction From Carbon-1 In *n*-Butanol By The Hydroperoxyl Radical Calculated By Coupled Cluster And Density Functional Theories And Multistructural Variational Transition-State Theory With Multidimensional Tunneling. *J. Phys. Chem. A* **2012**, *116*, 12206–12213.

(20) Seal, P.; Papajak, E.; Truhlar, D. G. Kinetics Of The Hydrogen Abstraction From Carbon-3 Of 1-Butanol By Hydroperoxyl Radical: Multi-Structural Variational Transition-State Calculations Of A Reaction With 262 Conformations Of The Transition State. *J. Phys. Chem. Lett.* **2012**, *3*, 264–271.

(21) Zhou, C.-W.; Mendes, J.; Curran, H. J. Theoretical and Kinetic Study of the Reaction of Ethyl Methyl Ketone with $H\dot{O}_2$ for T = 600Ű-1600 K. Part II: Addition Reaction Channels. *J. Phys. Chem. A* **2013**, *117*, 4526–4533.

(22) D′Anna, B.; Bakken, V.; Are Beukes, J.; Nielsen, C. J.; Brudnik, K.; Jodkowski, J. T. Experimental and Theoretical Studies of Gas Phase NO_3 and $\dot{O}H$ Radical Reactions with Formaldehyde, Acetaldehyde and their Isotopomers. *Phys. Chem. Chem. Phys.* **2003**, *5*, 1790–1805.

(23) Sivaramakrishnan, R.; Michael, J. V. Rate Constants for $\dot{O}H$ With Selected Large Alkanes: Shock-Tube Measurements And An Improved Group Scheme. *J. Phys. Chem. A* **2009**, *113*, 5047–5060.

(24) Aguilera-Iparraguirre, J.; Curran, H. J.; Klopper, W.; Simmie, J. M. Accurate Benchmark Calculation of the Reaction Barrier Height for Hydrogen Abstraction by the Hydroperoxyl Radical from Methane. Implications for C(n)H(2n+2) where n = 2 $\rightarrow$ 4. *J. Phys. Chem. A* **2008**, *112*, 7047–7054.

(25) Friedrichs, G.; Davidson, D. F.; Hanson, R. K. Direct Measurements of the Reaction $\dot{H}$ + $CH_2O \rightarrow H_2 + HCO$ Behind Shock Waves by means of VisŰUV Detection of Formaldehyde. *Int. J. Chem. Kinet.* **2002**, *34*, 374–386.

(26) Vasudevan, V.; Davidson, D. F.; Hanson, R. K. Direct Measurements of the Reaction $\dot{O}H + CH_2O \rightarrow HCO + H_2O$ at High Temperatures. *Int. J. Chem. Kinet.* **2005**, *37*, 98–109.

(27) Wang, S.; Davidson, D. F.; Hanson, R. K. High Temperature Measurements for the Rate Constants of C1Ű C4 Aldehydes with $\dot{O}H$ in a Shock Tube. *P. Combust. Inst.* **2014**, –.

(28) Vandooren, J.; Tiggelen, P. V. Reaction Mechanisms of Combustion in Low Pressure Acetylene-Oxygen Flames. *P. Combust. Inst.* **1977**, *16*, 1133–1144.

(29) Westenberg, A.; Fristrom, R. H and O Atom Profiles Measured by ESR in C_2 Hydrocarbon-O_2 Flames. *P. Combust. Inst.* **1965**, *10*, 473–487, Tenth Symposium (International) on Combustion.

(30) Li, H.-Y.; Pu, M.; Ji, Y.-Q.; Xu, Z.-F.; Feng, W.-L. Theoretical Study on the Reaction Path and Rate Constants of the Hydrogen Atom Abstraction Reaction of CH_2O with $\dot{C}H_3/\dot{O}H$. *Chem. Phys.* **2004**, *307*, 35–43.

(31) Xu, S.; Zhu, R. S.; Lin, M. C. Ab Initio Study of the $\dot{O}H + CH_2O$ Reaction: The Effect of the $\dot{O}H$ůůOCH_2 Complex on the H-Abstraction Kinetics. *Int. J. Chem. Kinet.* **2006**, *38*, 322–326.

(32) Li, Q. S.; Zhang, X.; Zhang, S. W. Direct Dynamics Study on the Hydrogen Abstraction Reaction $CH_2O + H\dot{O}_2 \rightarrow CHO + H_2O_2$. *J. Phys. Chem. A* **2005**, *109*, 12027–12035, PMID: 16366658.

(33) Eiteneer, B.; Yu, C.-L.; Goldenberg, M.; Frenklach, M. Determination of Rate Coefficients for Reactions of Formaldehyde Pyrolysis and Oxidation in the Gas Phase. *J. Phys. Chem. A* **1998**, *102*, 5196–5205.

(34) Jemi-Alade, A.; Lightfoot, P.; Lesclaux, R. A Flash Photolysis Study of the $H\dot{O}_2 + HCHO \rightarrow H_2O_2 + HCO$ Reaction between 541 and 656 K. *Chem. Phys. Lett.* **1992**, *195*, 25–30.

(35) Robertson, S. H.; Seakins, P. W.; Pilling, M. J. In *Low-Temperature Combustion and Autoignition*; Pilling, M., Ed.; Comprehensive Chemical Kinetics; Elsevier, 1997; Vol. 35; pp 125–234.

(36) Choudhury, T. K.; Sanders, W. A.; Lin, M. C. A Shock Tube and Modeling Study of the Methyl + Formaldehyde Reaction at High Temperatures. *J. Phys. Chem.* **1989**, *93*, 5143–5147.

(37) Bentz, T.; Striebel, F.; Olzmann, M. Shock-Tube Study of the Thermal Decomposition of CH_3CHO and $CH_3CHO + \dot{H}$ Reaction. *J. Phys. Chem. A* **2008**, *112*, 6120–6124.

(38) Taylor, P. H.; Yamada, T.; Marshall, P. The Reaction of $\dot{O}H$ with Acetaldehyde and Deuterated Acetaldehyde: Further Insight Into the Reaction Mechanism at Both Low and Elevated Temperatures. *Int. J. Chem. Kinet.* **2006**, *38*, 489–495.

(39) Farnia, S.; Vahedpour, M.; Abedi, M.; Farrokhpour, H. Theoretical Study on the Mechanism and Kinetics of Acetaldehyde and Hydroperoxyl Radical: An Important Atmospheric Reaction. *Chem. Phys. Lett.* **2013**, *583*, 190–197.

(40) da Silva, G.; Bozzelli, J. W. Role of the α-Hydroxyethylperoxy Radical in the Reactions of Acetaldehyde and Vinyl Alcohol with $H\dot{O}_2$. *Chem. Phys. Lett.* **2009**, *483*, 25–29.

(41) Khamaganov, V. G.; Bui, V. X.; Carl, S. A.; Peeters, J. Absolute Rate Coefficient of the $\dot{O}H$ + $CH_3C(O)OH$ Reaction at T = 287–802 K. The Two Faces of Pre-reactive H-Bonding. *J. Phys. Chem. A* **2006**, *110*, 12852–12859, PMID: 17125300.

(42) Katsikadakos, D.; Zhou, C.-W.; Simmie, J.; Curran, H.; Hunt, P.; Hardalupas, Y.; Taylor, A. Rate Constants Of Hydrogen Abstraction By Methyl Radical From *n*-Butanol And A Comparison Of CanTherm, MultiWell And VariFlex. *P. Combust. Inst.* **2013**, *34*, 483–491.

(43) Goldsmith, C. F.; Tomlin, A. S.; Klippenstein, S. J. Uncertainty Propagation In The Deriva-

tion Of Phenomenological Rate Coefficients From Theory: A Case Study Of n-Propyl Radical Oxidation. *P. Combust. Inst.* **2013**, *34*, 177–185.

Graphical TOC Entry